FINAL REPORT

AN EVALUATION OF AN ICCD IMAGER OF DYNAMIC RANGE EXPANSION TECHNIQUE AND APPLICATION OF INSITU PROCEDURES FOR LIFE-TIME EXTENSION

Contract # NAS-5-24305

Submitted to:

National Aeronautic and Space Administration

by

Douglas G. Currie

15 December 1979

Revised

22 February 1982

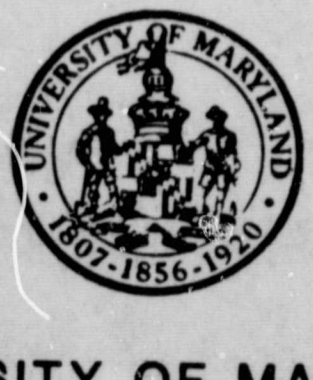

UNIVERSITY OF MARYLAND

DEPARTMENT OF PHYSICS AND ASTRONOMY

COLLEGE PARK, MARYLAND

FINAL REPORT

AN EVALUATION OF AN ICCD IMAGER OF DYNAMIC RANGE EXPANSION TECHNIQUE AND APPLICATION OF INSITU PROCEDURES FOR LIFE-TIME EXTENSION

Contract # NAS-5-24305

Submitted to:

National Aeronautic and Space Administration

by

Douglas G. Currie

15 December 1979

Revised

22 February 1982

UNIVERSITY OF MARYLAND

DEPARTMENT OF PHYSICS AND ASTRONOMY

COLLEGE PARK, MARYLAND

TABLE OF CONTENTS

TABLE OF FIGURES

I. INTRODUCTION

The work described in this report is a study of two important aspects of the research conducted at the University of Maryland toward a practical implementation of the Intensified Charge Coupled Device (ICCD) as a photon-counting array detector for astronomy. The first area of concentration was to determine the rate and extent of the lifetime-limiting damage to the CCD caused by the impact of high energy electrons, and to find whether various methods of annealing the damage were productive. The second effort was to determine the performance of the ICCD in a photon-counting mode to produce extended dynamic range measurements.

There are two main effects that appear as the practical results of the electron damage to the CCD. One is an increase in the "leakage current", i.e., the normal thermal generation of charge carriers in the silicon that provides a background "dark" signal that adds to the light-produced image. In an undamaged CCD, the leakage current is usually fairly uniform across the photosensitive area of the silicon chip, with the exception of various "bright" pixels which have an anomalous leakage current well above the overall level. As the accumulated exposure of an ICCD increases, the leakage current uniformity is gradually lost, as the brighter regions of the image on the CCD will suffer greater damage than the low-illumination portions. The second effect of the damage is a reduction of the full-well capacity of damaged pixels, a less serious effect for photon counting since normally the device is operated such that the pixels never approach satuation.

The principal mechanism of damage by electrons is the creation of charge pairs in the dielectric of the CCD. One of the components of a

charge pair is then attacted to the interface with the conducting electrode, where it becomes locked in place in the few hundred angstroms closest to the conductor. In addition, there may be problems due to structural damage of the silicon. This may result in charge traps which are formed at the silicon surface.

Various techniques may be employed to release trapped charges and hence anneal the damage. We have primarily studied the use of ionizing electrons in the absence of the normal CCD-operating electric field which attacts the holes to the interface. Also, we have obtained a reduction in the damge-induced leakage current through annealing by electron bombardment. Various other annealing methods have been noted, but without detailed study. The foremost among these is simple room-temperature annealing while the ICCD is idle. Although significant reduction in leakage current has been obtained this way, the constant upgrading of electronic support systems for the ICCD has made it difficult to maintain any absolute calibration, so this remains an interesting but currently ill-defined phenomenon. Two other procedures were not tested: first, ultra-violet annealing, which was not possible for the ICCD available since it did not have an UV-transmitting photocathode. Second was high-temperature annealing, which was considered too great a risk to use on an ICCD not specifically dedicated to such a procedure.

The second major area of concern in this report is the study of high dynamic range imaging with the ICCD. This required a great effort to actually achieve photon-counting with the system, as well as the development of a background subtraction procedure (in external hardware) to show that photon-limited performance could be retained even in the

presence of substantial electron damage to the CCD.

The photon-counting system was evaluated by comparison between the analog video output of the CCD and the photon discriminated output. A lack of proper performance of both of these modes prevented the final detailed intercomparison that was desired. The photon limited performance was limited by the data deconverter; new techniques are being implemented in order to correct this problem. At present, the difficulty has been isolated, and several fixes defined, from which the most promising will be chosen.

II. THE UNIVERSITY OF MARYLAND ICCD SYSTEM

The Intensified Charge Coupled Device, or "ICCD", used in the University of Maryland ICCD System, consists of a Fairchild CCD-202 solid state self-scanning image sensor placed in the electron image plane of an ordinary S-20 photocathode. The photocathode and the CCD are contained within an evacuated, cylindrical glass envelope. Photoelectrons emitted from the photocathode are accelerated towards the CCD by a potential difference of o15kv, and focussed on the CCD by an electrostatic focussing cone. The device is manufactured by the Elctronic Vision Company. The bonding of the CCD on a header to provide pins for external electrical connections is performed by Fairchild Corporation. Figure 1 is a drawing of the ICCD, in the latest cnfiguration as delivered by the Electronic Vision Company for this contract. A high permeability magnetic shield is also included, but is not shown in the drawing.

The basic principle of operation of the ICCD is that the accelerated electrons, which transfer the optical image (of an external source formed on the photocathode) to the CCD surface, create "packets" of charge carriers, typicaly 2000 carriers for each photoelectron, which are sufficiently large to be discriminated as "single photon events" against the normal CCD system readout noise, which is typically equivalent t about 100 carriers per ixel per scan. Thus the photoelectrons act as a light amplifier which permits the CCD to be used in a single photon counting mode, with direct application to high dynamic range imaging and to interferometry.

In normal operation, there is random, thermal genertion of carriers

within the photosites of a CCD that produces a characteristic "dark pattern" even with no external ilumination. The accumulation of these carriers, known as "leakage current", is linear with time at constant temperature, so that the average leakage current signal read out of the CCD should be inversely proportional to the scanning frequency that determines the length of individual exposures. Such behavior is illustrated in Figure 2. Figure 3 shows the dependence of the leakage current on CCD temperature.

This dark signal must, of course, be subtracted from the total signal for each scan of the CCD, for each pixel, in order to determine the net signal attributed to external illumination of the ICCD. The uncertainty in the determination arises from the (uncorrelated) addition of the fluctuations in the leakage current and the random noise associated with the readout electronics. At the scan frequencies and temperatures used in the University of Maryland system, the readout noise usually dominates the leakage current fluctuations. That the total random nise is independent of the ICCD accelerating voltage is demonstrated by Figure 4.

Figure 5 is a block diagram of the complete Mark IV (M IV) camera system and support electronics, including the following devices:

Video Data Procesor (VDP)--coordinates the camera clocking system located in the Remote Control Unit (RCU) with the primary data storage system, the Circulating Semiconductor Memory (SRCSM), which both provides the RCU with scan control logic and also stores the output camera images by adding successive frames to its internal memory.

The NOVA II field computer contains an analog-to-digital converter (ADC) plus a sample and hold (S&H) system that converts the incoming

video signal from the camera head into a digital data stream suitable for storage in the SRCSM.

The oscilloscope and the Tectronix 604 Monitor (driven by the video amplifier and synchronized to the SRCSM) provide real time output pictures for diagnosis by the operator.

The Thermoelectric Unit (TEU) provides temperature stabilization for the CCD, using a thermoelectric cooler coupled to the CCD with thermal grease.

The Local Power Unit (LPU) supplies the high voltage required for electron acceleration in the ICCD.

Finally, a second camera head (M III) is connected to the RCU, to provide the proper operating environment for the RCU, which was originally designed for two-camera interferometry applications.

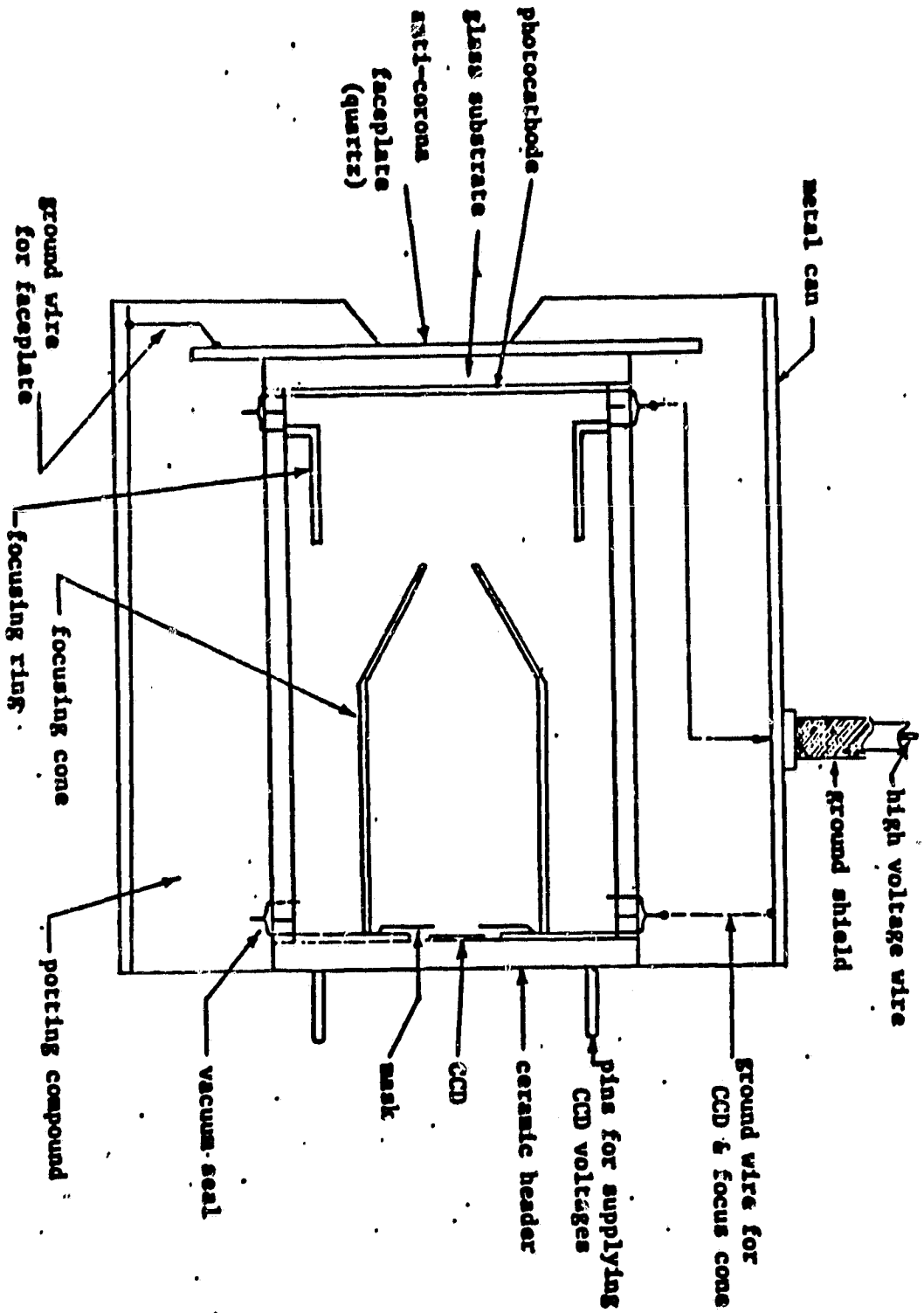

Figure 1. ICCD schematic.

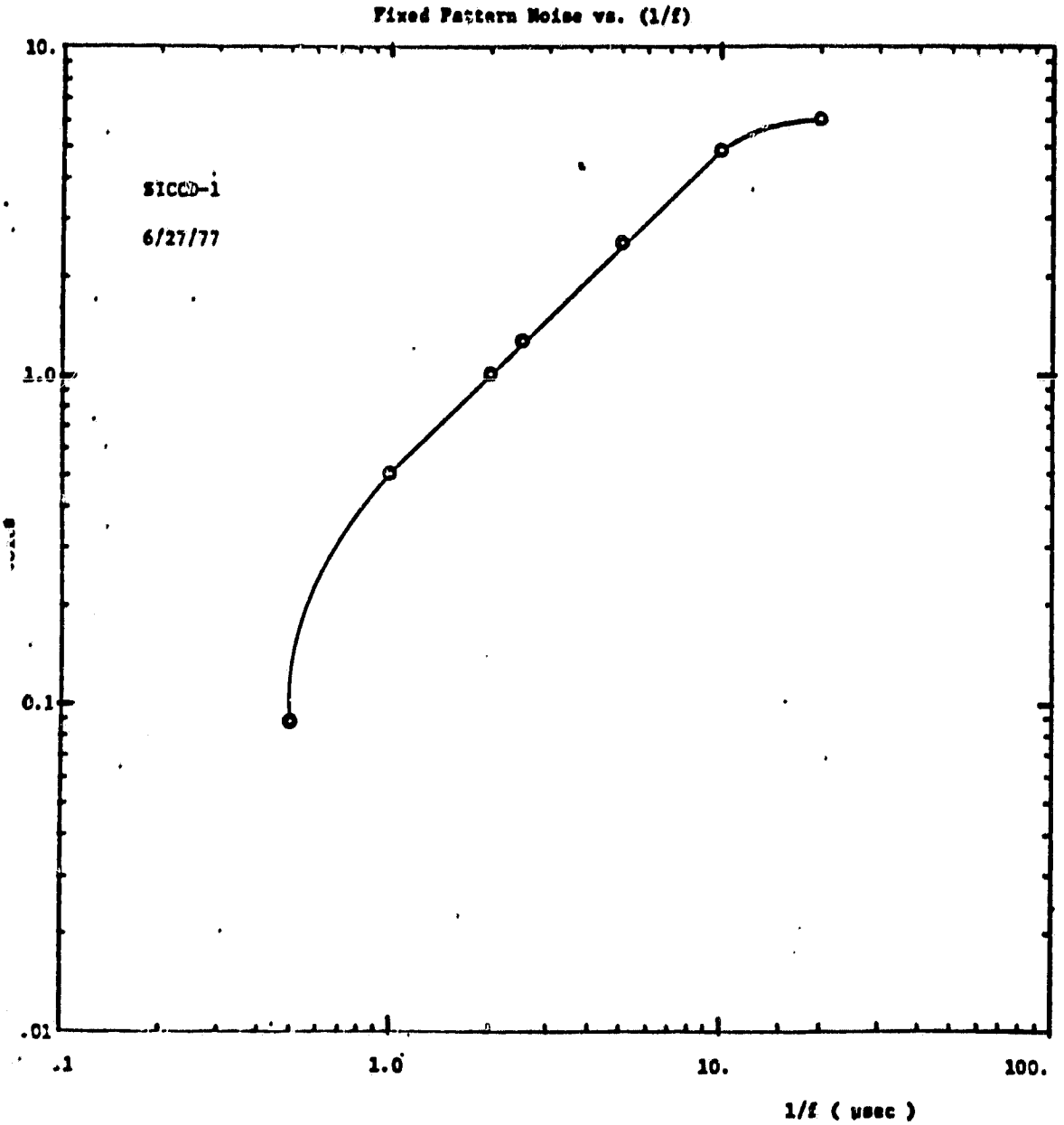

Figure 2. Frequency dependence of the dark current.

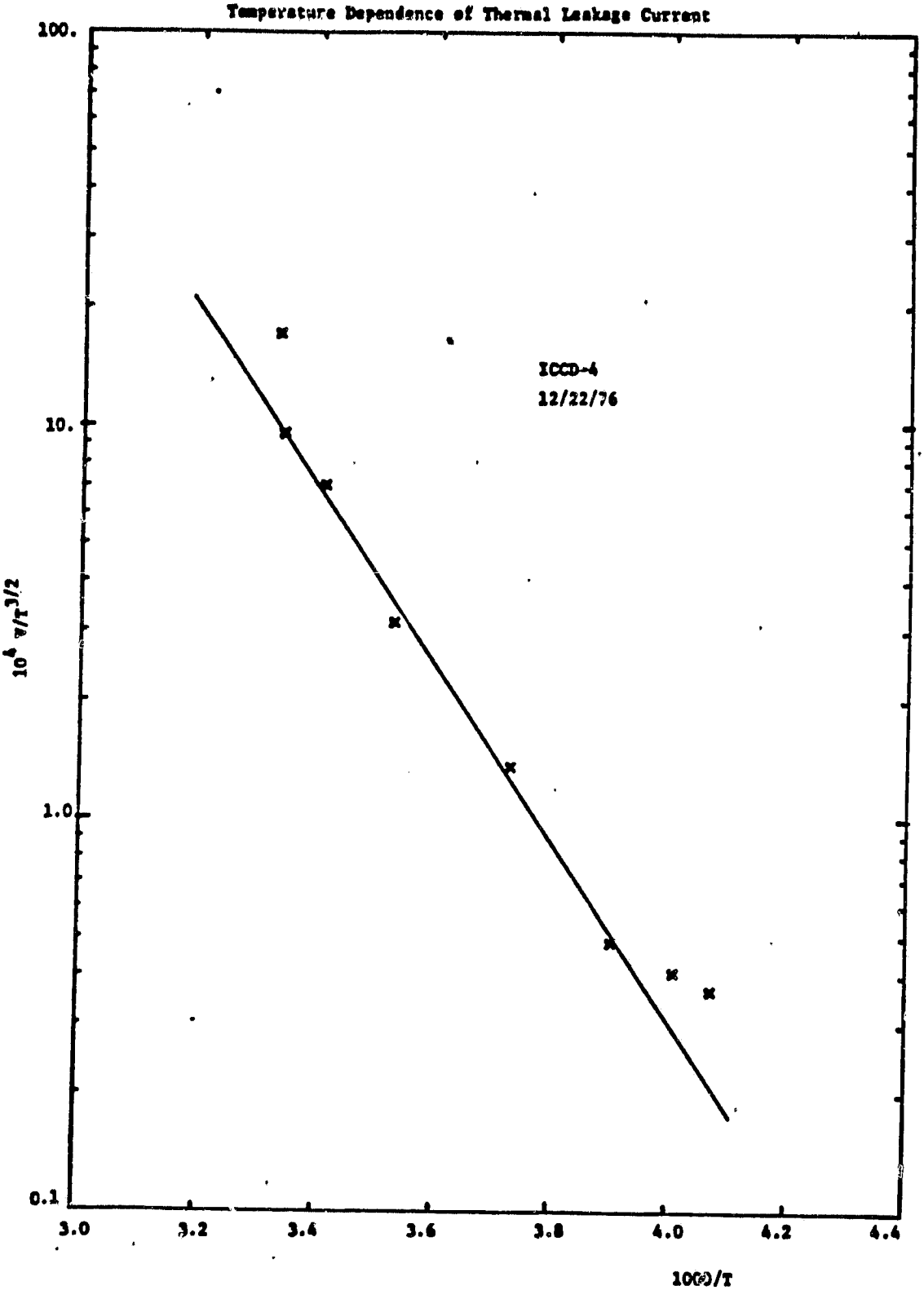

Figure 3. Temperature dependence of the dark current.

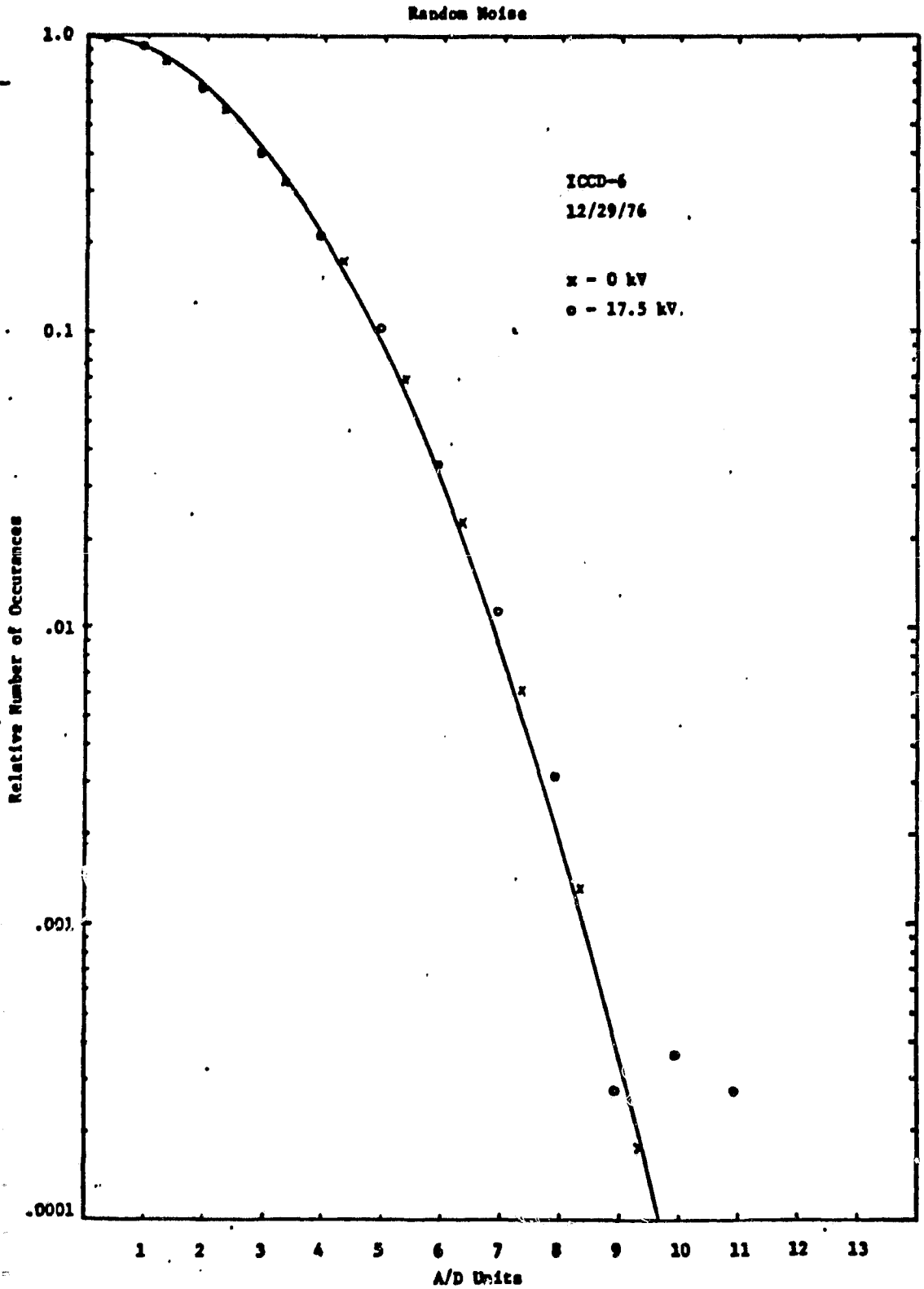

Figure 4. Effect of high voltage on the random noise.

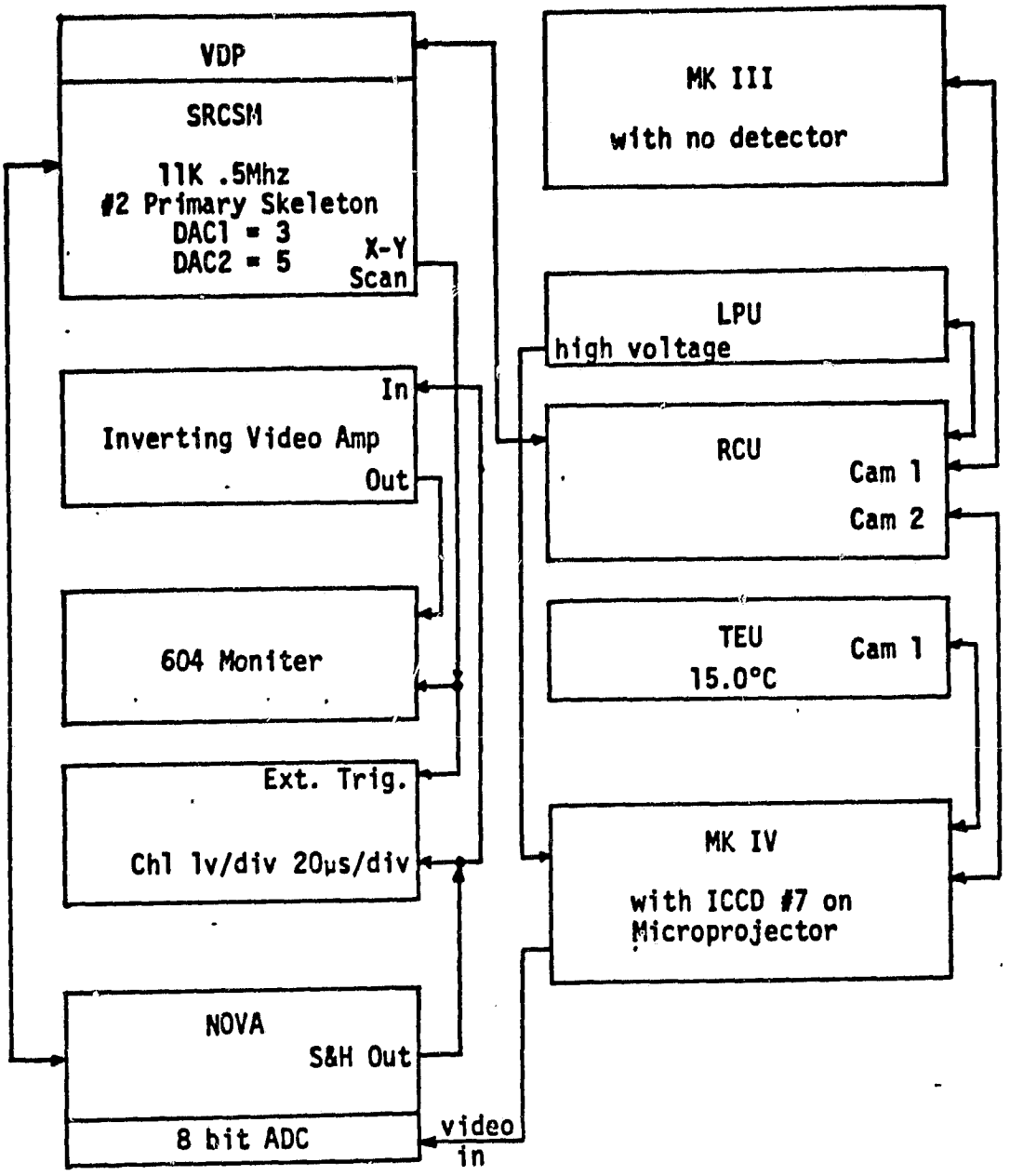

Figure 5 - Block Diagram of Damage and Annealling Test

III. MEASUREMENTS OF DAMAGE AND ANNEALING PERFORMANCE

A. The Proposed Damage Evaluation

The damage evaluation procedure suggested in the proposal consisted of the following steps:

1. Record the leakage current at a reference temperature with active temperature controls.
2. Illuminate a limited region of the photocathode so a region of about 30 x 30 pixels is irradiated.
3. Record the irradiation level using the SSDRS.
4. Record total leakage current after the completion of the irradiation.
5. Illuminate the CCD with light at two intensity levels with the accelerating voltage turned off. The date from the low level illumination will be used to evaluate changes in sensitivity from one pixel to the next. The high level illumination will be used to evaluate any changes in full well capacity.
6. Return to step 2 and repeat this sequence until the excess leakage current becomes significant in magnitudes.

Several modifications to the above procedure proved to be necessary. Most of these arose from the circumstance that the ICCD was delivered at the very end of the contract period. In addition, the delivered ICCD failed on the first application of high voltage. However, a test ICCD was made available by the Electronic Vision Company; this device had an extremely low quantum efficiency but was quite uitable for the damage measurements. The results described in the remainder of this report were obtained with this ICCD, henceforth referred to an "ICCD 7."

B. Previous Damage Measurements

We now review tests of ICCD electron damage conducted prior to this contact.

The first efforts to measure damage wee conducted at the Electronic Vision Company, using a University of Maryland-supplied CCD. The glass protective cover on the CCD was removed and replaced with a mask containing 5 holes. One hole was used as a control, while the others were successively uncovered t expose a region of the CCD to bombardment to 15 kv electrons. The irradiated chip was analyzed at the University. The results were primarily qualitative, but showed that the ship would still image satisfactorily, if the proper background "dark image" were subtracted. Moreover, the fact that regions above and below the damaged regions imaged equally well indicated that the transfer efficiency of the damaged pixels was unimpaired.

More precise results were obtained with the first ICCD, ICCD-1. This tube was operated at 15 kv and exposed to flashes of light from an LED. The aount of damage was controlled with the width and repetition rate of the pulses driving the LED. Dark patterns were recorded before and after each exposure of the CCD to the LED light. The results, shown in Figure 6, revealed that a total exposure of 4.5×10^4 photoelectrons per pixel would produce an increase in average leakage current equivalent to the signal produced by one photoelectron. This equivalence is, of course, dependent on the scan rate, since higher scan frequencies provide shorter exposure times in which the leakage current signal accumulates. For the ICCD-1 tests, the scan rate is 44 frames per second.

Figure 7 shows the results of a damage test conducted with ICCD-6, which used one of the newer CCD-202 devices rather than the CCD-201 used in ICCD-1. The most noticeable feature of the figure is the highly linear relationthip between excess (i.e., resulting from damage) leakage current and total exposure. The slope of the line corresponds to a dark signal increase of one photoelectron equivalent signal per second.

A second CCD-202 ICCD, ICCD-4, was tested for damage at an accelerating voltage of 18 kv. These results were less reliable than the preceding tests due to experimental difficulties, but the resulting damage rate was found to be 1 photoelctron equivalent signal per 1.9 x 10^5 incident photoelectrons, at 44 frames/second.

Table 1 summarizes the results of the damage tests. The figures have been normalized to a common CCD scan rate of 50 frames per second. It may be observed that the CCD-201 is more susceptible to damage than the CCD-202, which most likely arises from a structural difference between the two devices. The newer CCD-202 has a thicker overlying register structure than the CCD-201, so that photoelectrons entering the CCD-202 lose more energy before entering the underlying silicon. The table also shows that higher accelerating voltage produces more damage, which is consistent with a model of dark current enhancement being proportional to the amount of energy deposited in the silicon.

We can use the above results to estimate a useful lifetime for an ICCD used in a typical astrnomical application. Suppose the cameras are run at a designed data rate of 2 Mhz, i.e. 175 frames per second, and assume further that the array is subscanned, i.e., only a portion, n x m pixels, is shifted out of the array at a time. The tubes will be

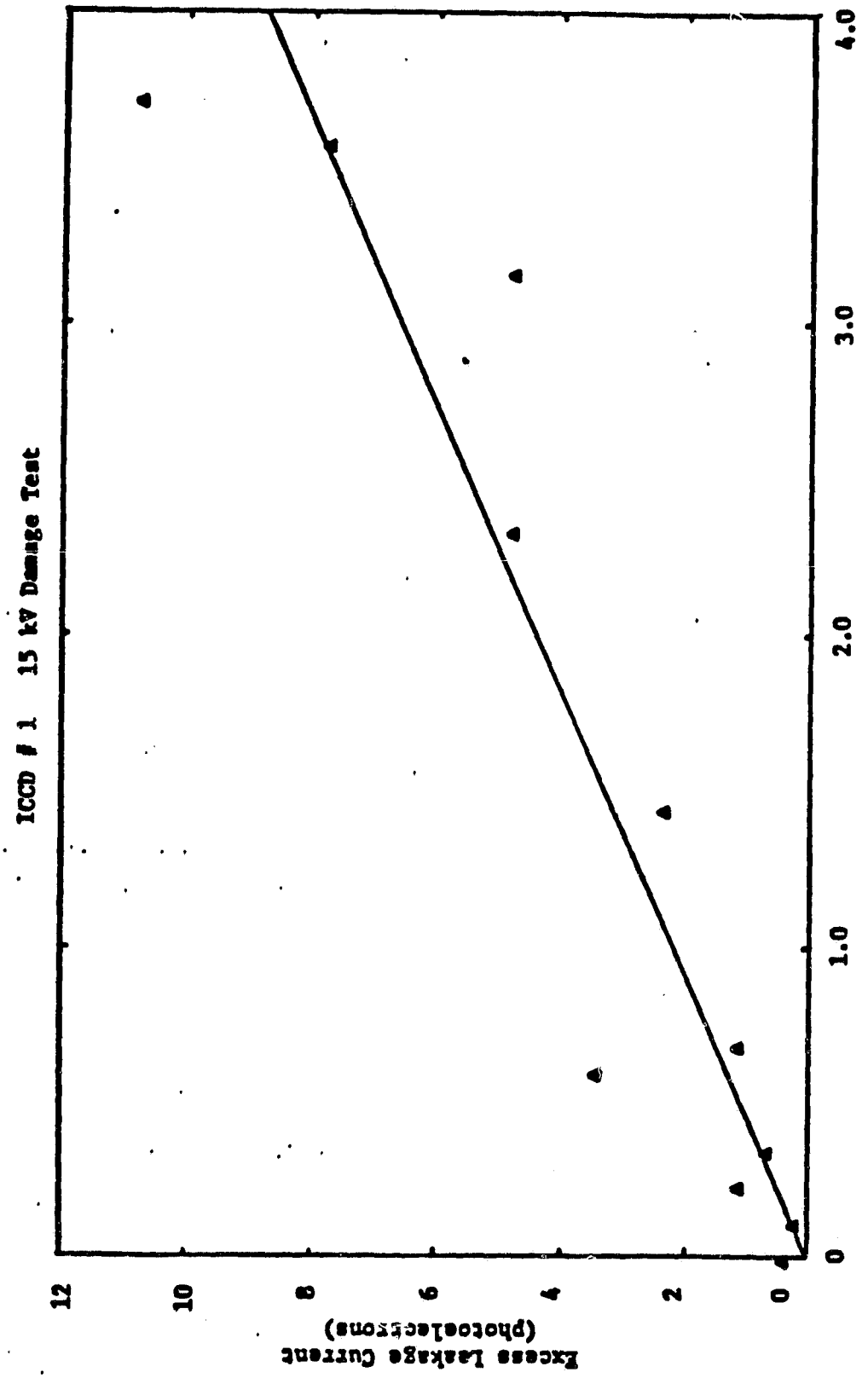

Figure 6. Damage test using a CCD 201.

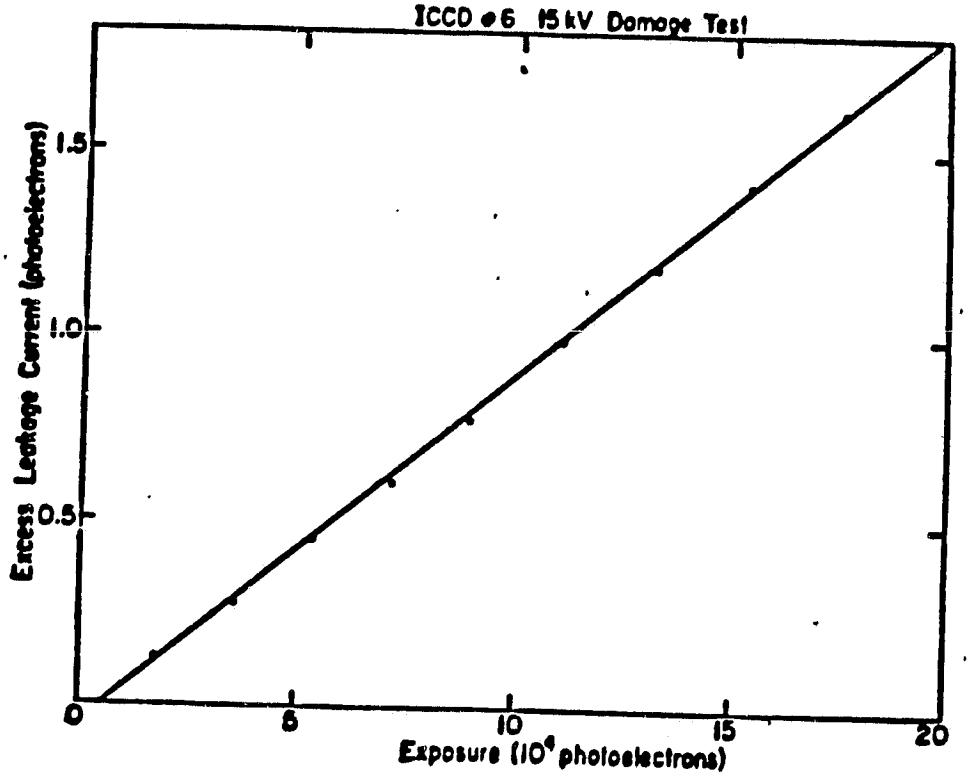

Figure 7. Damage test using a CCD 202.

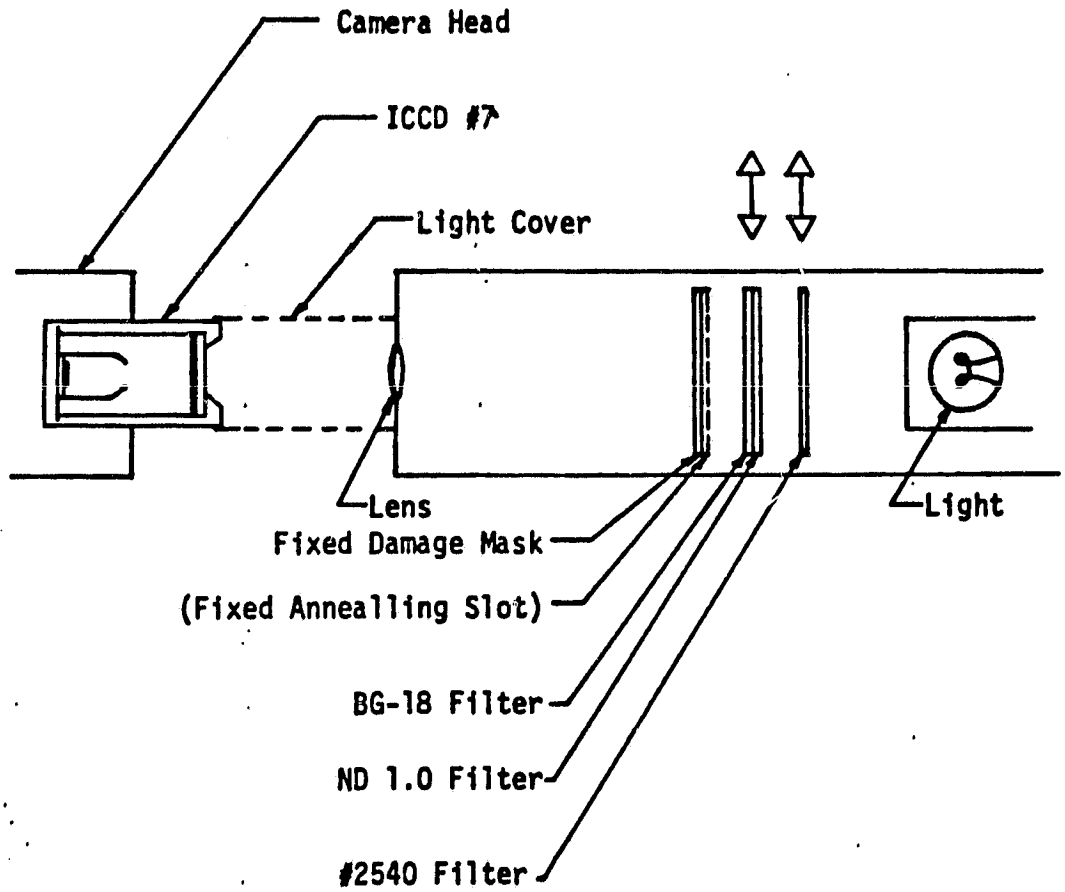

Figure 8. Microprojector Arrangement for Damage and Annealling Tests

TABLE 1

Type of CCD	201	202	202
ICCD #	1	6	4
Voltage	15	15	18
Damage Exposure* (10^5 pe)	0.51	1.1	2.1
Date of Test	6/29/75	9/17/76	10/25/76

* Normalized to a data rate of 50 frames per second; this is the total exposure required to increase the leakage current by an amount equivalent to the average signal from one photoelectron per scan.

operated at about 0°C, to further reduce the leakage current, typically by about a factor of 8. Taking from table 1 a representative damage figure of 10 photoelectrons per pixel per scan to produce a one photoelectron equivalent dark current increase, the above considerations would reduce the damage rate to

$$8 \times (175/50) \times 100/n) \times 100/m) \times 10^5 .$$

For $n = m = 10$, this dosage is 2.8×10^8 photoelectrons. At typical count rates of 100/second, the dosage corresponds to 3 months' observing at eight hours per night, so we conclude that the damage problem is not too seere for this type of application.

C. Current Damage Measurements

A systematic investigation of ICCD damage effects was planned and performed for this contract. Two preliminary damage test runs and one preliminary annealing test were carried out, followed by the primary damage test, and finally the annealing test. Extensive data was taken and analyzed, including a complete set of sensitivity data.

The experimental arrangement shown in Figure 8 was chosen so that the tests could be made in one continuous run with a minimum of adjustments. This eliminated any possible sources of error; for example, the light source was turned on and adjusted to an appropriate level prior to data taking, and left untouched for the entire run. All intensity control was then provided by insertion or removal of optical filters.

The damage tests were done by exposing the CCD array to bombardment by 15 kv electrons at a constant rate, and periodically recording the frames. Each test, performed without interruption, took four hours and forty-five minutes, accumulating 30 data records. Each individual dose

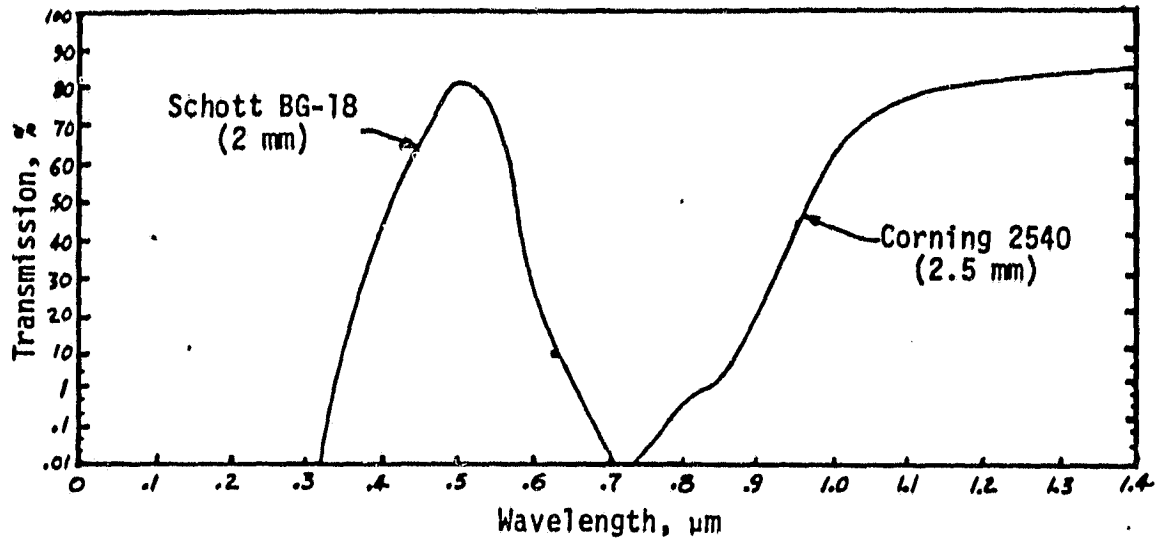

Color Glass Filters

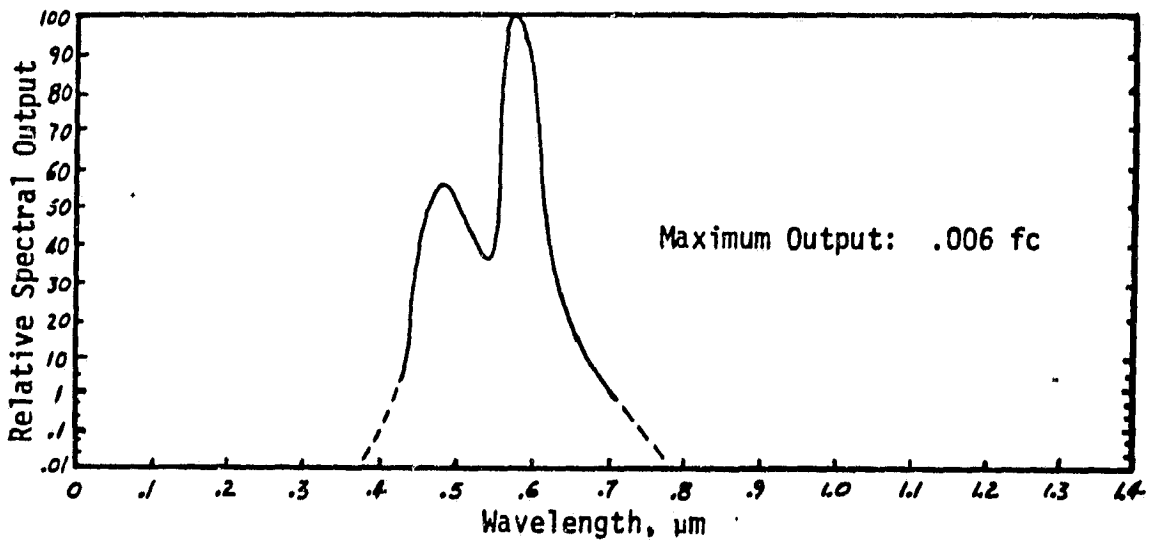

Low Light Level Source of Microprojector

Figure 9. Spectral Curves for Filters and Light Source of Microprojector

increment was three minutes, with the last several sets receiving ten minute exposures. Due to the low photocathode sensitivity, it proved to be difficult to measure the actual intensification gain, so that the dose rate in photoelectrons was uncertain, lying between 10 and 70 photoelectrons per pixel per scan. These values are based on an independently measured on-chip amplifier gain. This rate is quite high compared to anticipated levels in astronomical use of the ICCD. In the subsequent discussion, ilumination levels will simply be expressed in "ADU" (Analog-to-Digital Units), as they are recorded in the data sets. The conversion is very close to 1 ADU = 0.01 volts.

An area of the CCD exhibiting a relatively uniform leakage current pattern was selected for damage exposure. A mask was made, consisting of two sets of four small apertures, each of which exposed a 10 x 10 pixel area of the CCD, with about a 10 pixel separation between the apertures. Neutral density filters were placed over the apertures so that each set of four apertures consisted of an ND 0.0, ND 0.5, ND 1.0, and an ND 1.5 filtered aperture as shown in Figure III.12. By selecting nearby unilluminated areas for comparison, the increase in leakage of the area exposed by the apertures could be obtained.

Two color glass filters, used to control the incident light intensity, were placed in the filter holders of the microprojector. A two millimeter thick Schott BG-18 with an ND 1.0 filter was in one holder, and a Corning 2540 filter, 2.5 millimeter thick, was in the other. As can be seen by their transmission shown in Figure 9, when both filters were in the optical path essentially all the light from the thermal source was blocked. With only the BG-18, the photocathode would receive the focused image of the aperture mask. With only the Corning

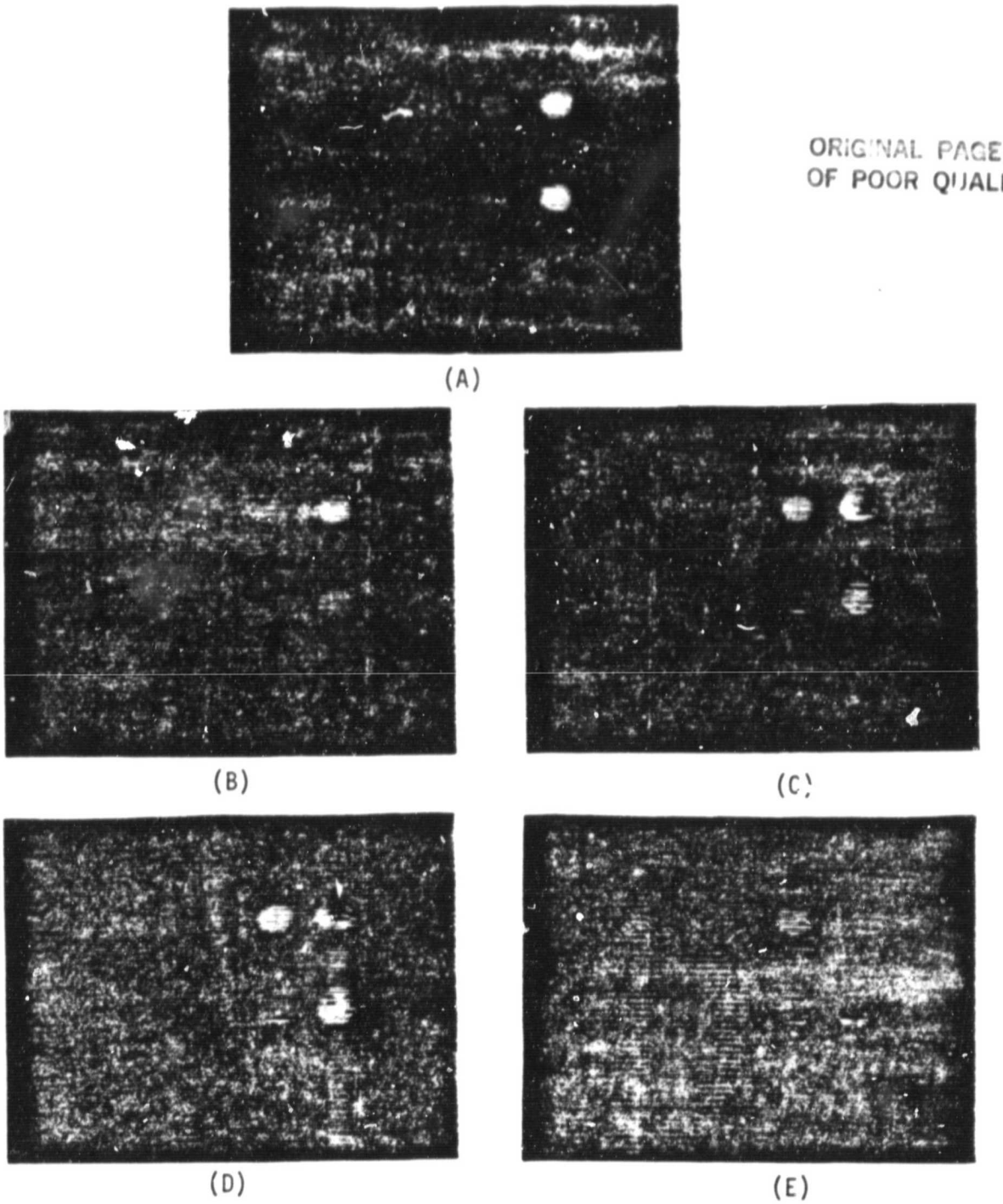

Figure 10 Damage and Annealling Test. (A) is the photoelectron image at start of test. (B) is the damage after 180 seconds. (C) is the damage after 4925 seconds. (D) is the damage after 6867 seconds. (E) is the damage at the end of the test (11,427 seconds).

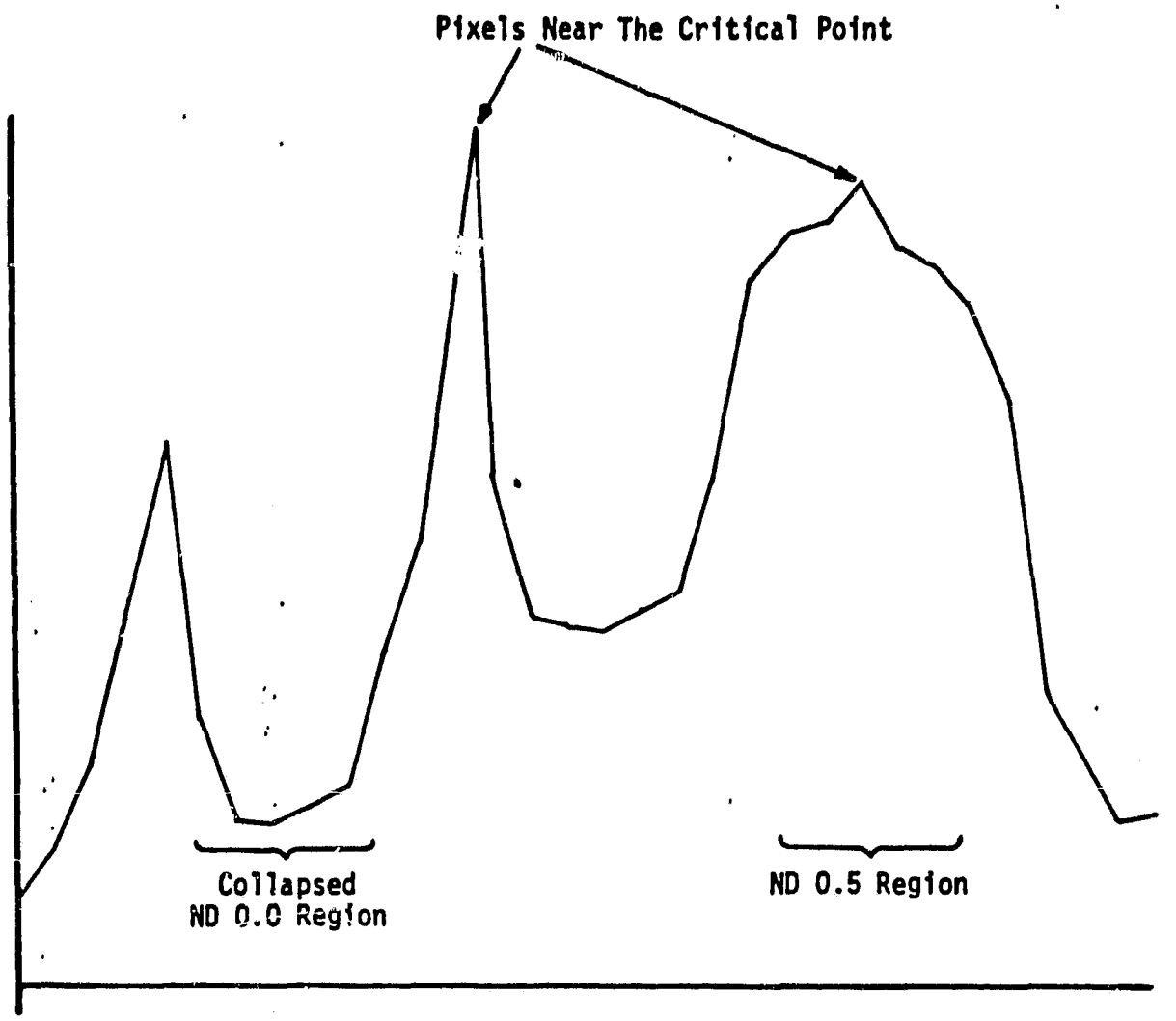

Figure 11. Line Profile of Damaged Regions in a Fairchild 202 CCD

2540, however, the photocathode would not respond, and the red filtered light would illuminate the CCD array itself with an unfocused image. The red response of the array would produce a sizable signal in this light. Thus by recording a set of frames first with the green (BG-18) filter alone, then with the green plus the red filter, then with the red filter along, and repeating this after each increment of the total damage dose, it was possible to obtain for each ND filter aperture area the damage, the dose, and the sensitivity of the CCD.

During the first part of the primary damage test, conducted 10/26/78, the leakage current increased linearly with dosage as expected. However, with continued exposure, the rate of increase slowed, then stopped. Further damage dose caused the leakage to drop abruptly, going down past the original pre-test levels to a near-zero leakage charge accumulation level. This occurred on an individual pixel basis, but once the levels had dropped, a pronounced smearing effect was observed in the respective vertical columns. Figure 10 shows computer generated pictures from the original data tapes. Picture (A) in the figure shows the photoelectron image of the aperture mask. Picture (B) is the difference between two dark images taken before and after 180 seconds of damage dose. Picture (C), (D), and (E) show the accumulated damage at 4,925, 6,867, and 11,427 seconds. In picture (C), note the dark pixels in the most heavily damaged region. These have just passed the critical point and are rapidly falling in amplitude. Picture (D) shows the pattern with one area completely collapsed. Picture (E) shows the damage pattern at the end of the damage test. The vertical smearing is readily apparent. This smearing effect dominated the ND 1.0 and ND 1.5 regions, as it occurred before significant damage had taken place in

the low illumination. Figure 11 is the profile of the line through the collapsed region.

The date was analyzed initially by selecting 5 x 5 pixel squares centered in the regions of interest, and averaging the intensity in each square. Later, the same line provile was taken frm each run and a single pixel in each of the ND 0.0 and the ND 0.5 regions on the line extracted. The same procedure was applied to the annealling data as well. The results of the 5 x 5 array processing, and the single pixel data, are shown in the figures discussed below.

Earlier work (Killiany, 1974; Silzars, 1974; Tull, 1975) had produced appaently ambiguous results. Most workers agreed that at very low doses the damage was linear. However, there were some reports of an upper limit which was conjectured to mean that eventually a saturation limit would be reached, and that no further damage would occur beyond this limit.

Figure 12 shows the single-pixel damage curves. It is appaent that all the reported effects occur The linear region is followed by a region of decreasing slope, and then a section where the damaged area's leakage remains constant and, in fact, begins to decrease in some instances.

Beyond this point, the damage increases again. It reaches a critical level which is clearly dependent on the total dose, and crops rapidly thereafter to very low levels where it reamins constant. The sensitivity, as shown by Figure 13, is reduced by a factor of six at and beyond the critical level. The leakage can drop wth increasing dose, but the damage is increased, as evidenced by the sensitivity curve. There is a maximum level of the leakage, but, again not of the damage

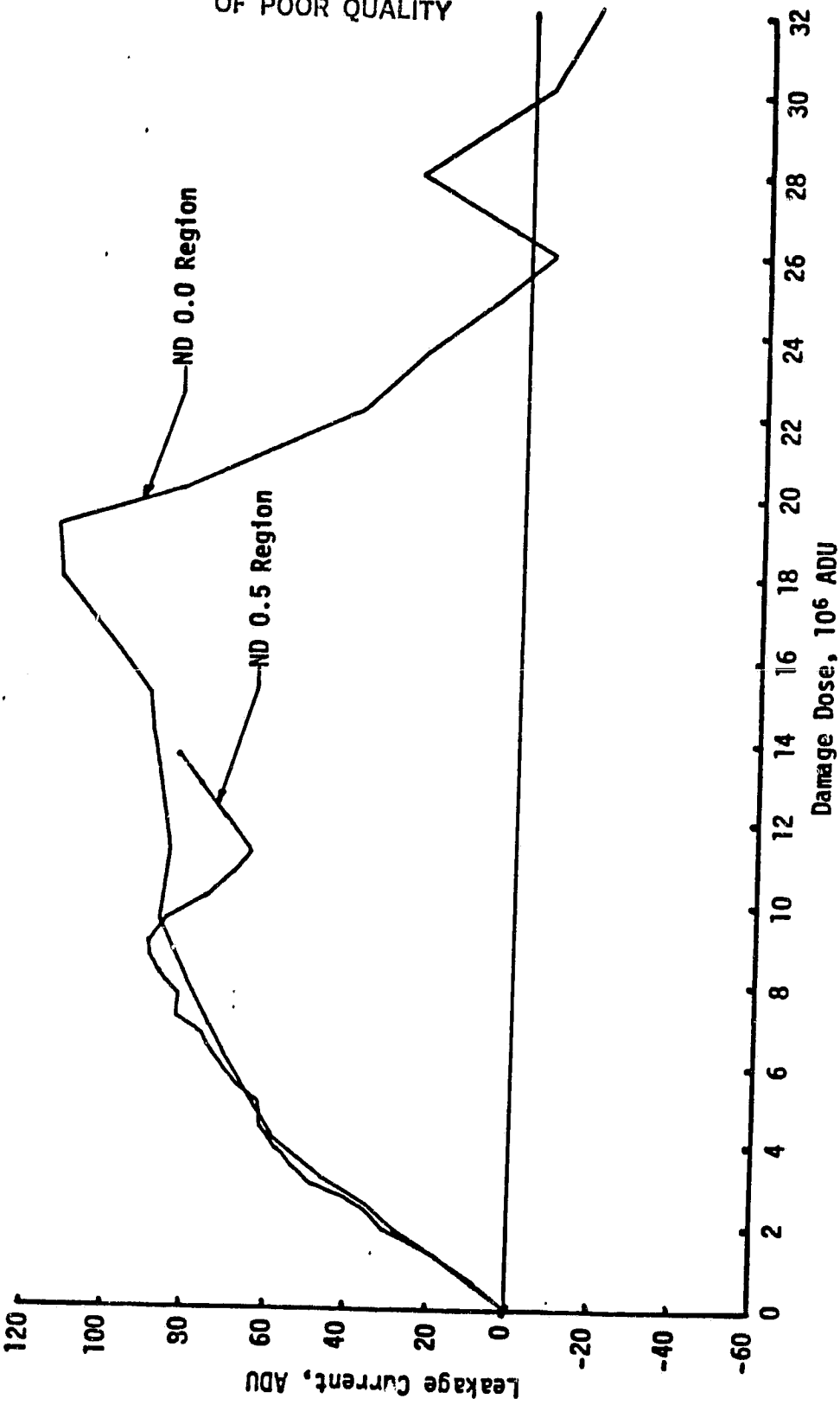

Figure 12. 15 kv Photoelectron Damage of Individual CCD Pixels

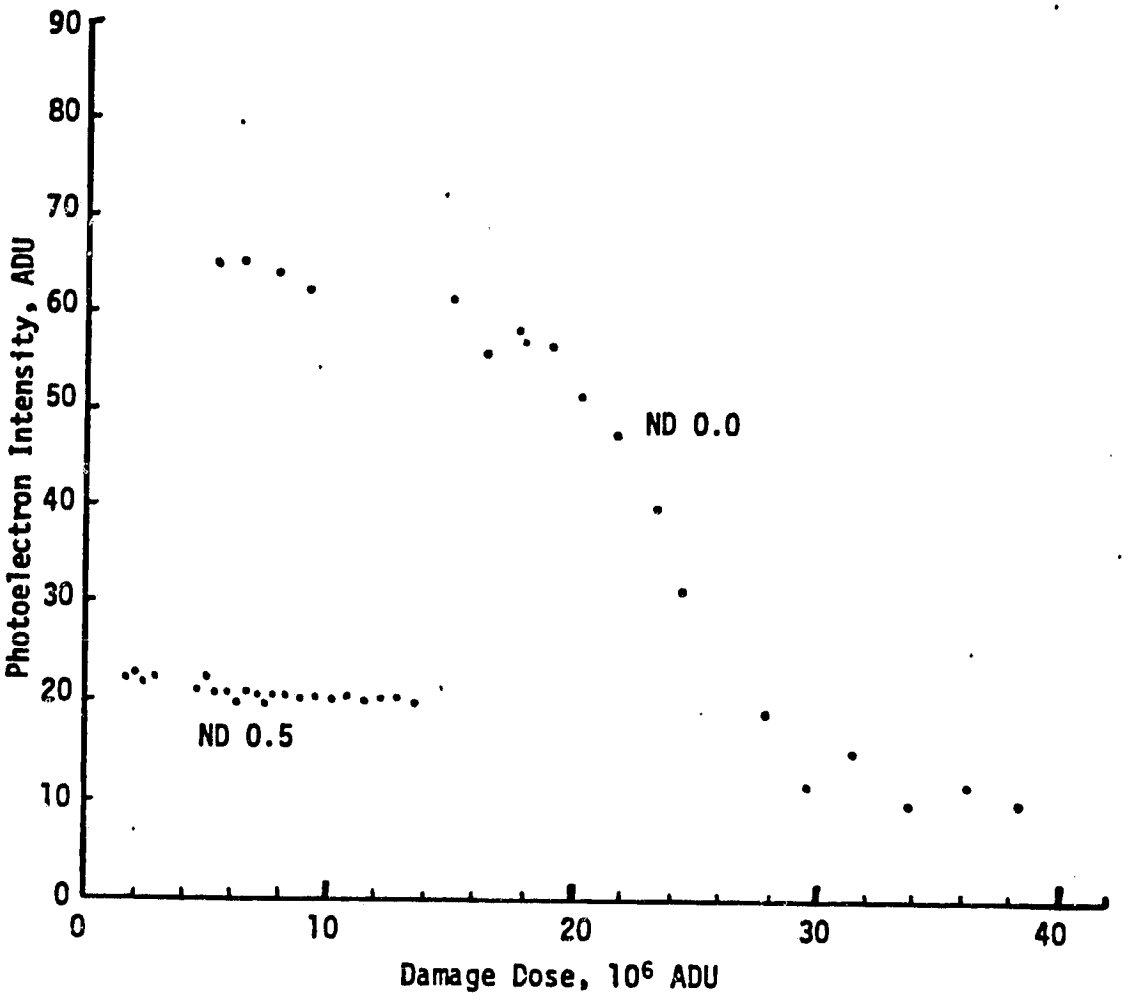

Figure 13. Response to Photoelectrons as a Function of the Total Damage Dose

suffered by the chip.

In Figure 14, the four curves obtained by using 5 x 5 pixel areas are sown, and the single pixel date is replotted for comparison. The close agreement of the single pixel curves and those for ND 0.0b and 0.5b shows that the damage behavior is consistant for different intensity levels and for different vertical and horizontal alignments of the areas that were damaged. For ND 0.0a, the curve has a slower initial damage rate, but does not level off, and thus reaches the critical level at approximatey the correct total dose. The curve for ND 0.5a is quite different than the others, but still follows the general trend.

The slow rise of the ND 0.0a curve could be due to the fact that in the 5x5 region some ixels had received a greater or leser total dose than the rest. This is due to: 1) there was a small amount of prior damage to the irradiated areas, although the most nearly uniform region was chosen for the tests; and 2) the light invensity profile across the unmasked aperture of the microprojector has a significant decrease outward from the optical axis. This is due to the non-lambertian surface of the frosted light bulb used as the thermal source. For these reasons, it is felt that the single pixel curves are somewhat more accurate than the array-average curves.

There are six phases of damage as a function of total dose. The initial phase exhibits a linear slope This is shown quite clearly in the composite graph of Figure 15. Following the linear region, however, the leakage increases more and more slowly with dose. The next region is a transition. The type of damage in phase two appears to saturate. During this transition, the leakage increases slightly, if at all, and

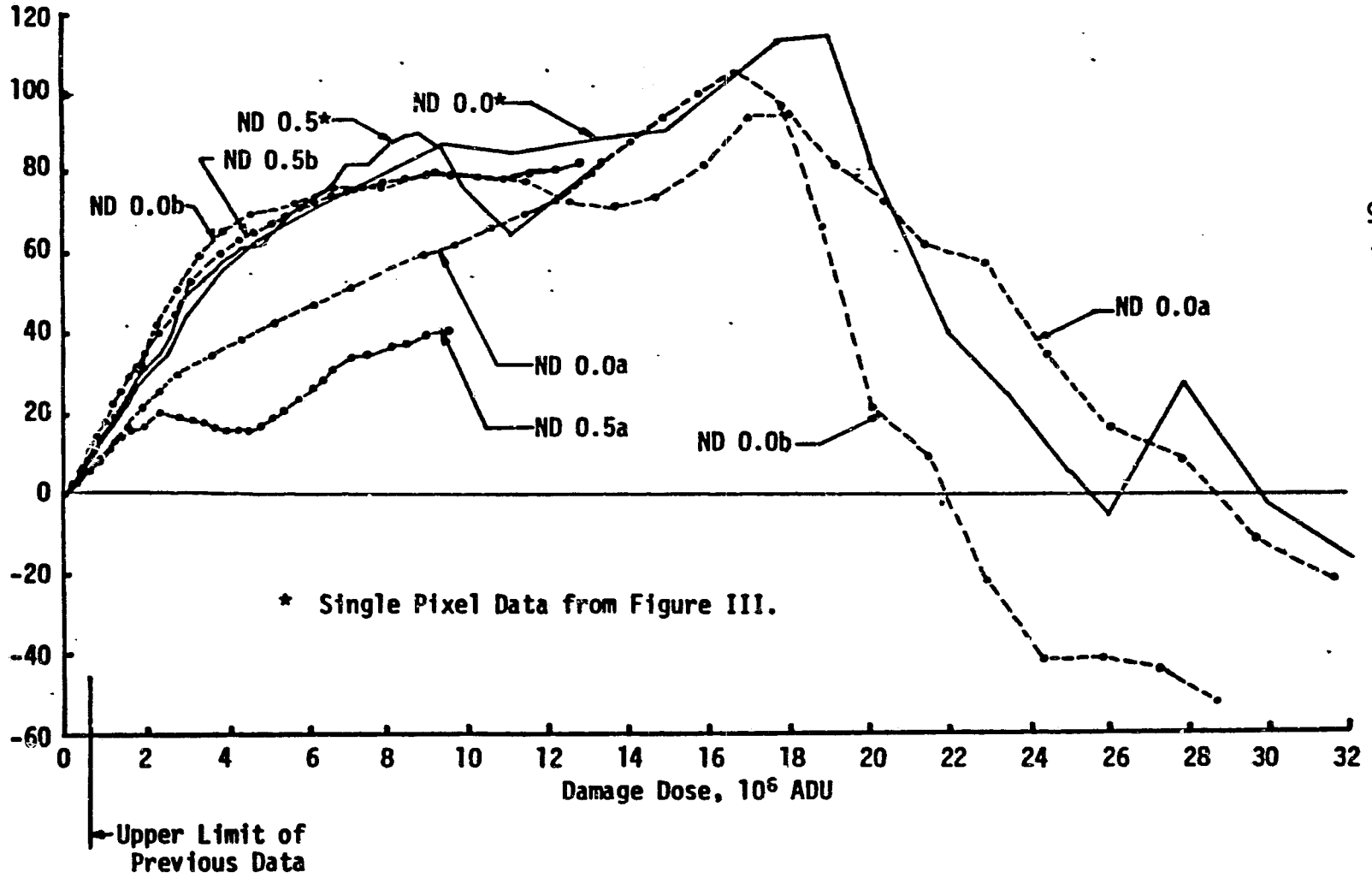

Figure 14. 15 kv Photoelectron Damage to a CCD

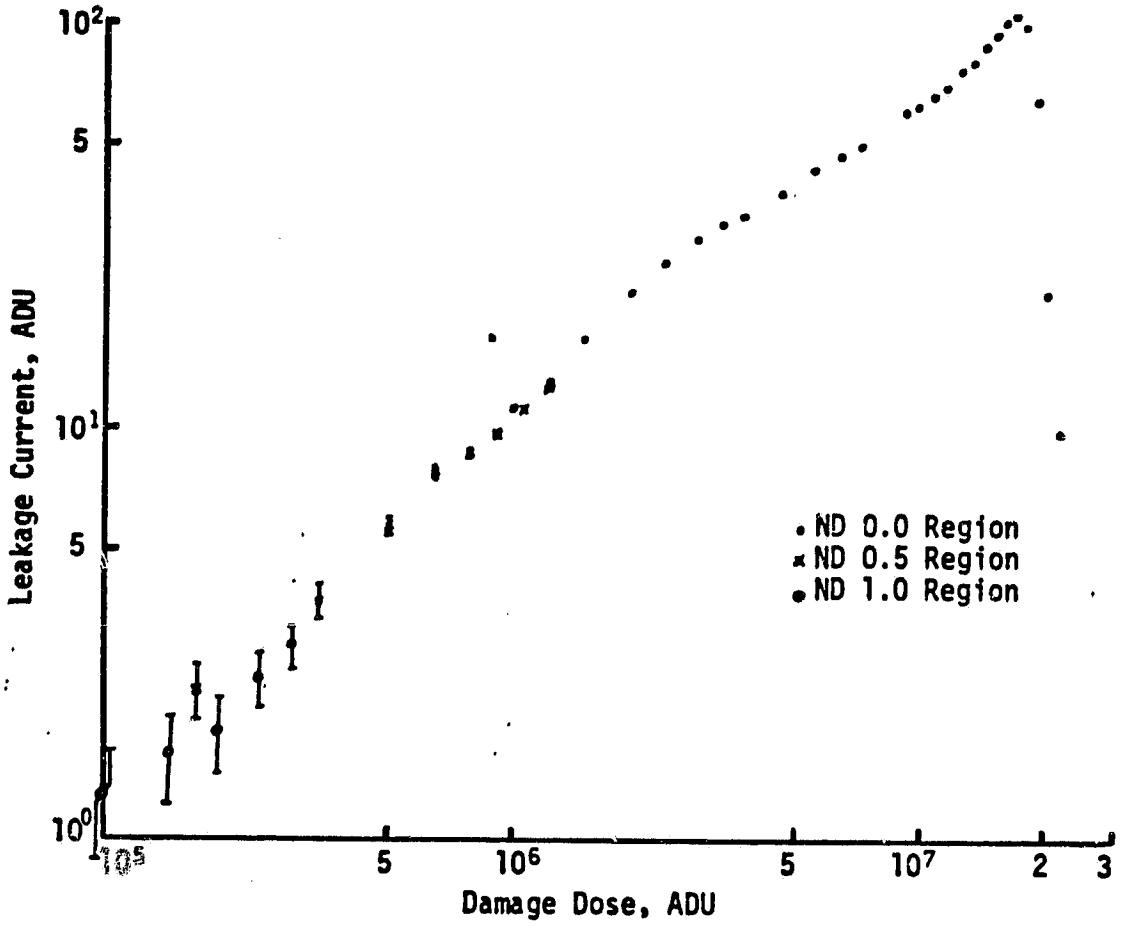

Figure 15. Composite Graph of Damage for Three Intensity Levels

may decrease slightly.

The fourth region is characterized by a more or less linearly increasing leakage level, at about one half the rate of region one. A very rough extrapolation shows that this linear slope could intersect the origin. The sensitivity is more or less constant in these first four regions.

The fifth region is the sudden drop of both the magnitude of the leakage current and the sensitivity of the affected pixels. This is clearly the region where the amount of damage has exceeded some threshold limit for retention of the charge packets by the CCD.

The sixth region is where the leakage current and the sensitivity level out and do not change with increasing dose. There may be additional regions beyond the dose limit of these measurements.

A possible mechanism that would produce the observed behavior is the same type of damage occurring at the same time in different parts of the CCD structure. Thus the overall behvior would be a single process repeated on different scales. Most of the curves in Figure 14 separate neatly into a component that peaks at about 10×10^6 ADU and a larger component that peaks at 20×10^6 ADU. If this is the case, then since the sensitivity is unchanged at 10×10^6 ADU, the lower component of the damage must take place in a part of the photosite that does not affect the charge confinement ability.

The effects of annealling are shown in Figure 16. The annealling was done by removing the driver pulses from the CCD and then duplicating the exposure used in the damage test. These exposures were also conducted at 15 kv. A slot mask, rather than the 4-aperture mask, was used in order to include previously undamaged regions. The amplitudes

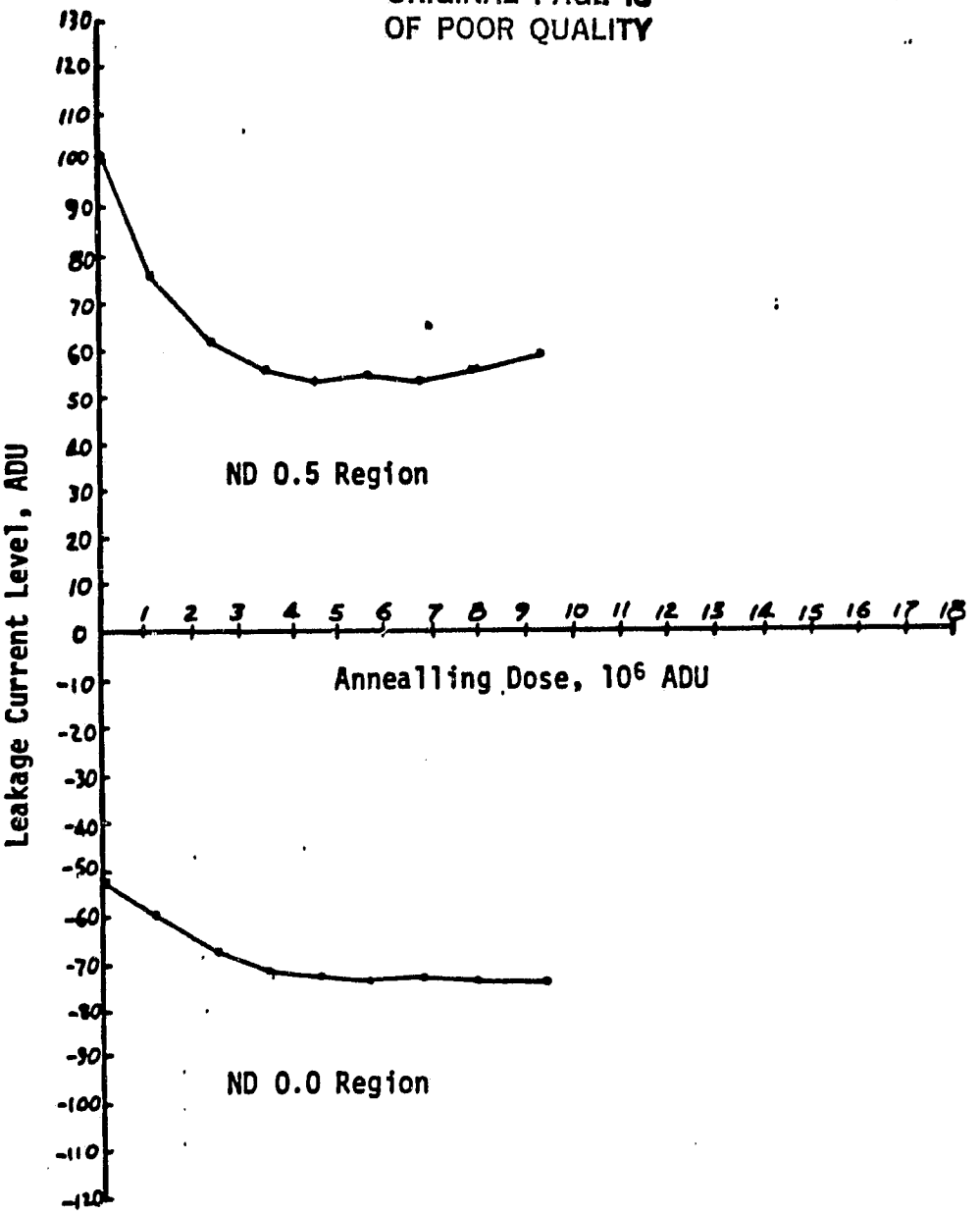

Figure 16. 15 kv Photoelectron Annealling of CCD

of the driver pulses (the clock voltages) were not changed from their values at the start of the damage and annealling tests.

The CCD annealed at approximately one-third the rate at which it damaged for the same dose. Those areas which had passed the critical point were not annealed. The annealing reversed after a dose approximately equal to one-fourth the critical dose.

The tests showed that the sensitivity of damaged pixels on either side of the critical point did not show a dependence on the incident illumination. This implies that at least to the intensities used, the pixels has not reached their full-well depths. If they had, then an increase in intensity would have shown a drop in the sensitivity as the excess carrier electrons were lost.

D. Other Annealing Methods

One mechanism for the reduction of the accumulated charge at the dielectric/electrode boundary is thermal diffusion during intervals when the CCD is unused. This will proceed at some, somewhat slow, rate at room temperature. This effect has been ovserved in our studies, as well as the effect of an increase in leakage current shortly after the damage. However, the detailed measurement of such annealing over a several week or month period has been in sharp conflict with the requirements to upgrade the performance of the ICCD camera head and the data recording system. In order to obtain the necessary long baseline, the system must be left undisturbed in order to not change its calibration. This has not been possible, and the attempts to calibrate through system changes have not been successful on a highly quantitative basis. There is a reduction in damage due to thermal leakage, but this appears to be a multi-week effect for a 1/e improvement. Even a multi-

month interval has not led to total elimination of the enhanced leakage pattern, but it has led to (apparently) very significant reductions. The study of this requires a very stable knowledge of clock voltages since the magnitude of the pattern, and the effective gain of this system depends in detail on the clock voltages.

Exposure of the ICCD to high temperatures would presumably increase the annealing rate by speeding the rate of diffusion of charge carriers within the CCD. However, this procedure does pose a significant risk to the photocathode and hence could not be attempted on the borrowed ICCD which was used for the other tests.

Some work at Fairchild has indicated that the use of ultraviolet light may serve to anneal some of the exces leakage current. However, this requires that the ICCD have a face plate which is transparent to ultraviolet light. This was not included in the final funding of this research, so these tests were not possible.

IV ICCD FABRICATION

E. Recent Experience with the Intensified CCDs

As has been indirectly mentioned in the earlier discussion, there has been a significant difficulty in the fabrication and delivery of the ICCD's by the Electronic Vision Company. The tests which were to be conducted under this contract were significantly hampered by the lack of the delivery of ICCDs which were expected. Two ICCD fabrication starts were supported by NASA, one under this contract and one under a separate earlier contract. The result of these two tube starts has been one marginally operational tube. Thus the testing program has required significant reconfiguration in order to permit as much data as possible to be obtained. We will now consider the ICCDs which have been used in some of these tests.

Magnetic ICCD

A magnetically focussed ICCD using a Fairchild CCD 202 was obtained from Dr. Robert Hobbs of the Goddard Space Flight Center. This tube has been used in a joint UM/GSFC program which has resulted in an extensive test series and a number of observations. Initially this tube showed a good quantum efficiency but there were significant numbers of ion events, which would indicate this tube was gassy. With time the quantum efficiency has gradually degraded. The variation in the leakage current across the CCD has always been sufficiently high that this CCD has never been suitable for photon counting; however, it has worked very well in the analog recording mode. The leakage current in the CCD is now sufficiently high that electron annealing should be considered.

ICCD 8

This electrostatically focussed tube was the result of a tube run

by Electronic Vision Company on 24 March 1978 and was delivered in May 1978. Immediately after fabrication at EVC, this tube showed a gradual decrease in quantum efficiency indicating the possible presence of gas in the tube. However, the decrease in quantum efficiency leveled out to some degree and the tube was shipped to the University of Maryland. The CCD was tested and performed quite suitably. After a series of tests the high voltage was turned on. At an accelerating voltage of about 7 kv, an internal arc occurred, which destroyed the proper functin of the CCD.

ICCD 9

This is also an electrostatically focussed ICCD. Its quantum efficiency remained high in tests at the Electronic Vision Company. The CCD was tested and performed well, with a few bright pixels and generally flat background. The accelerating voltage was then applied and gradually raised. At about 13 KV, a background of photocounts, which gradually increased, was noted. This rapidly formed a bright, highly exposed spot, stil with no light input, so the acceleration voltage was turned off. This behavior is indicative of gas. The CCD continued to operate, apparently normally. When the accelerating voltage was turned on later, this phenomena did not repeat. Discussions were held with Electronic Vision but it is still not clear what caused this sequence of events.

The results were a decrease in the quantum efficiency of the photocathode by two orders of magnitude, and the formation of mildly damaged spot on the CCD, i.e., a region in which the leakage current had increased due to the heavy electron exposure. This area may be seen in the upper left region of the exposure if the discriminator levels are

set in a certain manner.

F. General Status of the ICCDs

We now consider the status of the existing ICCD fabrication and procedures.

Summary of Difficulties

There appear to be two primary difficulties in the devices which have been fanricated. The first problem is "leaks" of some types (real or virtual) which permits gas to enter the tubes. The second area of concern, at least on some earlier tubes which were fabricated by the EVC for another program, was field-emission corona. This was thought to be due to metallic burrs within the tube, and has apparently been solved by a design change.

Fabrication of Digicons

The Electronic Vision Company has recently been fabricating Digicons for use on the Space Telecope program. In this program several improvements have been made on the designs for the two-inch tubes bodies which are used for the magnetically focussed devices. The most recent series of twelve Digicons for the FOS project have all been free of gas and the photocathodes have (except for one in the extreme ultra violet) maintained high quantum efficiency. The fabrication of this series of Digicons has involved a number of changes in EVC procedures for Digicon fabrication. EVC is now implementing these changes in the procedure for the fabrication of the one-inch electro-statically focussed tubes which were used for the ICCD's.

Fabrication of the Quadrant Guider Tubes

The Electronic Vision Company expects to fabricate a number of quadrant guider tubes. These devices have the same one-inch tube body

as the ICCD and have a less critical diode assembly. These will be fabricated for various customers and should permit the evaluation of the new design changes. Following an evaluation of these results and this yield, an ICCD could be fabricated with a much higher confidence level, particularly if one of the guider tubes is tested with an excesively high voltage.

Other Possible Developments for ICCD

Several other approaches may be considered within this program. Some examples of these consist of:

1. Larger CCDs

The Fairchild Corporation fabricated larger CCD's with a larger number of elements. These are currently being investigated. These devices should operate on the University of Maryland electronics systems with only minor modification.

The performance of the UMAP system with these 244 by 190 and 488 by 380 devices should be essentially the same as the performance with our present CCD's.

2. Thinned Fairchild CCDs

The Electronic Vision Company is currently experimenting with Fairchild arrays which have been thinned for back-illumination. However, this venture is still at an experimental stage which does not imply a high realiability of obtaining a good tube. In addition, although back-illumination will reduce the "damage" or leakage effects of the photoelectron bombardment, it significantly changes the procedure for the photon counting operation. Since the transfer registers are no longer shuttered, one must now operate an electronic shutter beyond the photocathode (which may imply a low

duty cycle) and one must sweep the charge from the transfer registers before normal clocking. (Note that the "servo" data may be useable.)

3. Other Charge Coupled Device Arrays

At present, based upon the published values for the magnitudes of "read" noise, only the Fairchild Corporation CCD and the Texas Instruments CCDs seem to be of interest for photon counting operating. Most of the work for low noise work at Texas Instruments has been for data readout rates which are too slow for photon counting although it should be possible to increase this rate. Further, the thinned arrays will need some type of shutter since the transfer registers are not protected.

V. BACKGROUND SUBTRACTION

This section discusses a special technique developed at the University of Maryland to compensate for the difficulties in a photon counting system caused by the enhanced leakage current. Preliminary tests which have been conducted on such a system will be discussed.

Concept of Circulating Semi Conductor Memory

The original proposed form of the University of Maryland Array Photometer (UMAP) using an ICCD presumed the use of a fixed level discriminator in order to provide the single photoelectron discrimination. This approach has difficulty, that is, as the electron bombardment and camera head damage increases, the leakage current caused by this damage may in some cases rise above the discrimation level and thus trip the discriminator. This will be a performance-limiting effect at a rather low dose (10^8 per pixel). In the original concept, this required the cooling to 0°C or somewhat lower.

Proposed Upgrade

In order to eliminate this problem, it was proposed that the value of this leakage current for each individual pixel be stored in a separate memory. Thus, the value for each pixel would then be brought to the camera head in order to provide a signal to subtract from the signal from the CCD. The difference should then have a mean value of 0 and should show the single photoelectrons with much greater ease.

Implementation of Tests

In order to evaluate this technique, a series of tests were performed processing data from the CCD in the computer. Thus, the CCD output for a dark background was recorded many times. The many samples from a single pixel were averaged and this was used to establish the

value of the background. Frames were then recorded for which there were single photoelectron inputs. Within the computer, these background frames were then subtracted from the frames with single photoelectron inputs. The resulting pixel outputs were organized into a pulse-height distribution. The distributions showed a clearly separated single photoelectron peak, demonstrating the general validity of the technique. The procedure was successful even on dark background patterns corresponding to heavily damaged tubes. This permits us to infer that a real time hardware implementation of the subtraction process would be a suitable lifetime extension technique. A sample pulse height distribution for the experiment discribed above is shown in Figure 17.

As discussed earlier and implied by the above , a method of subtracting the leakage current pattern in real time would greatly enhance the practicality of the photon-counting ICCD system. A laboratory test was done to determine the existence of any unforseen problems. A software program which performs discrimination on an array had been in operation for some time. Using this after subtraction is the logical equivalent of the subtraction and discrimination on CCD data. It had shown that the technique would give completely satisfactory results of the subtraction was done. Many pictures showing single photoelectron discrimination of images were made with This software program has been used.

An image of the dark leakage pattern of ICCD #6 was recorded and put in a SRCSM memory track, and subtracted from the video output at the camera head. The subtracted signal was fed back to the head and through the discrimination circuits and the result monitered at the SRCSM

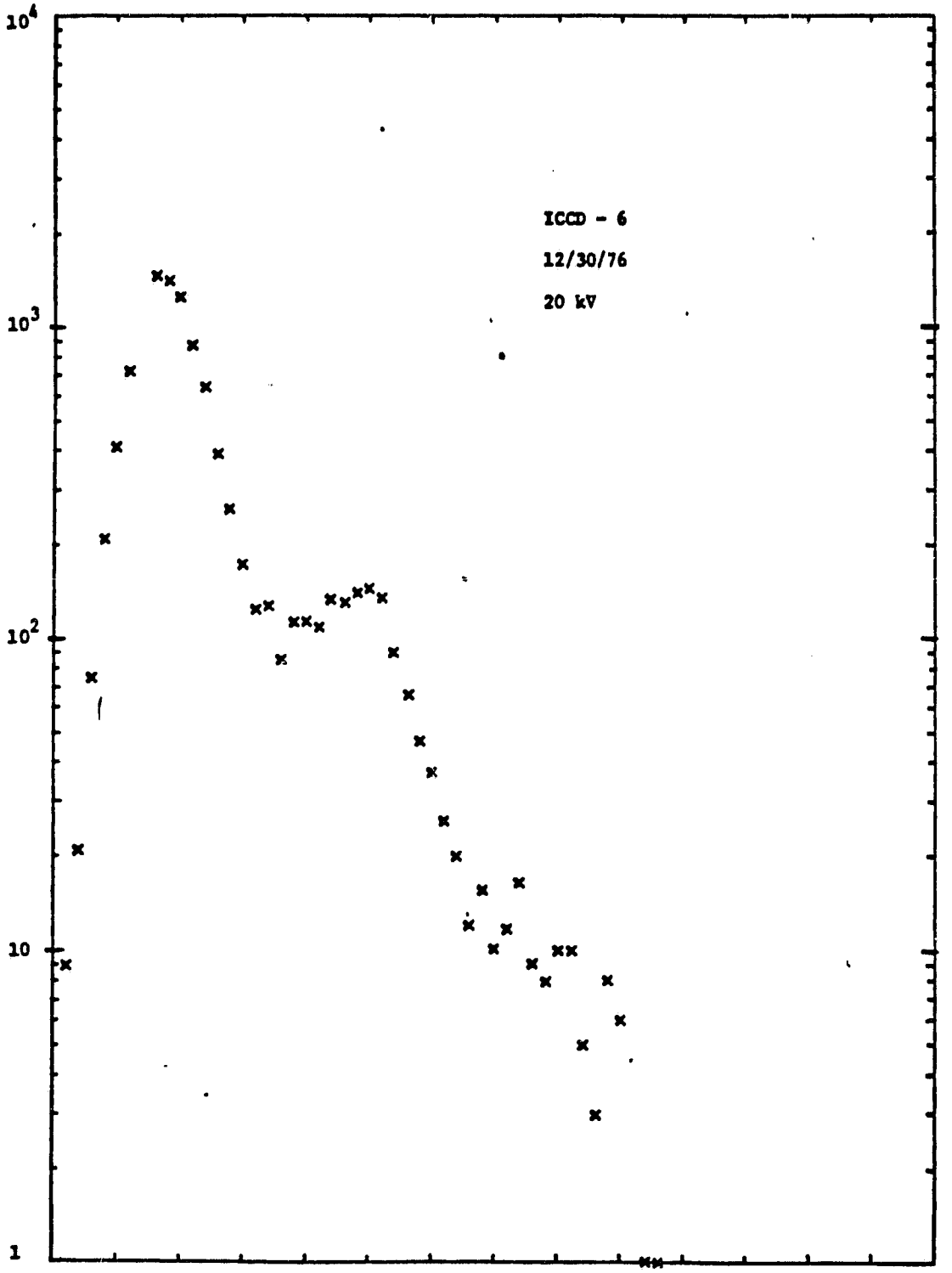

Figure 17. Dark-subtracted Pulse-height Distribution

output. All major pixel registration and synchronization adjustments were done, the only problem being that the unequal lengths of shielded cable carrying the video signals showed up as spikes at the end of each pixel. However, a substantial amount of pickup was observed, and it was concluded that a separate low noise subtraction circuit would be desirable. Figure 18 shows the subtracted and unsubtracted pictures.

The leakage current pattern on ICCD #6 consists of a burned-in image of a test chart. Careful examination of picture (A) in Figure 18 will show that there are several overlapping burned-in patterns of the test chart. It is emphasized that picture (A) is the dark leakage current pattern due to damage, not to a picture projected on the tube at the time of this test.

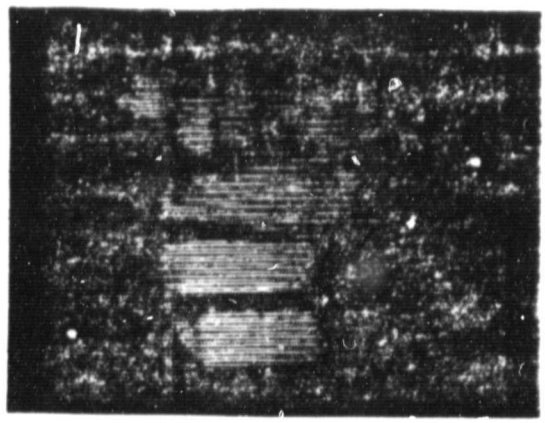

(A)

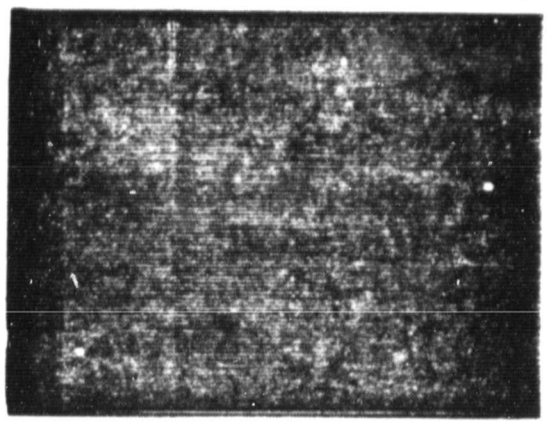

(B)

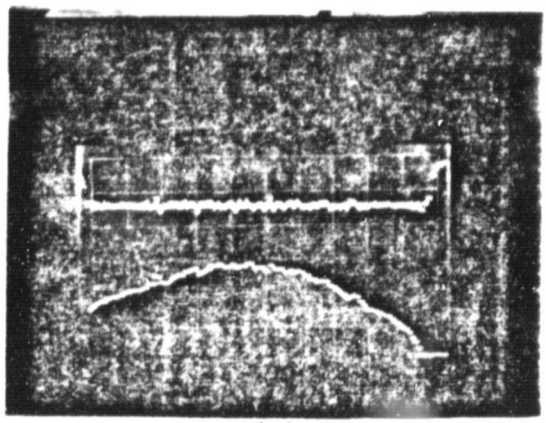

(C)

Figure 18 Real Time Dark Subtraction. (A) shows the original dark current pattern. (B) is the same video signal after subtraction. In order to show the residual dark pattern, there was no light imaged on the chip. (C) is a subtracted (upper trace) and unsubtracted (lower trace) line across the two images.

VI. TELESCOPE TESTS AND DYNAMIC RANGE

In this section, we discuss the general results of recent telescope operation and other field demonstrations of the performance of the University of Maryland Array Photometer (UMAP).

A. Astronomical Use of the UMAP System

1. Earlier Telescope Tests

The early tests of the UMAP on various telescopes were addressed primarily toward general calibration and evaluation. The list of individual tests and some further discussion has already been presented elsewhere. This was discussed on page 86 of the original proposal. This will not be further addressed in this document.

2. Recent Observations using the UMAP

The recent observations at the Hale Observatories have used the ICCD as the secondary observing instrument, when seeing and cloud conditions were such that the primary instrument, i.e., the Amplitude Interferometer, could not be used. These observations were of several types:

(a) Direct imaging mode

Most of the observations have consisted of direct imaging on the 200-inch and the 60-inch telescopes at Palomar Mountain. During different observing sessions, we have used both the magnetic ICCD and the electrostatic ICCD #9. The resolution of the ICCD systems, as used on both the 200-inch and the 60-inch telescopes, is about 2 pixels/arc-second.

(b) Spectrophotometric mode

The observations on the most recent trip also included the use of the Cassegrain prism spectrograph developed by J. A. Westphal. This was used with a resolution of 15 '/pixel. The system also imaged an extended field of about 60 arc-seconds in the spatially resolved imaging direction.

3. Astrophysical Objectives of the UMAP Observing Program

The thrust of the initial program for the use of the UMAP has been concentrated in two areas:

(a) Active galactic nuclei

The subject of this work is test observations of QSO's, BL Lac objects, N galaxies and Seyfert galaxies. Exploratory observations, both spectroscopic and direct imaging, have been made on representatives of each of these classes. An example of the spectrophometric observation appears in Figures 19 and 20. Figure 19 is 3C273 imaged with the imaging orientation such that the slit is in the direction of the jet. The system was set so that the spectral direction was not parallel to the row or columns, to value a systematic error. Within the computer, this image was then rotated so that the spectral direction is parallel to the edge of the ham. This is displayed with a linear quantization in Figure 20.

(b) Planetary Nebulae and H II regions

The study of planetary nebula and H II regions will also use several different modes of observation in conjunction with the UMAP system. In some of the brighter lines the entire nebula will be imaged. Our observation is in such a line shown

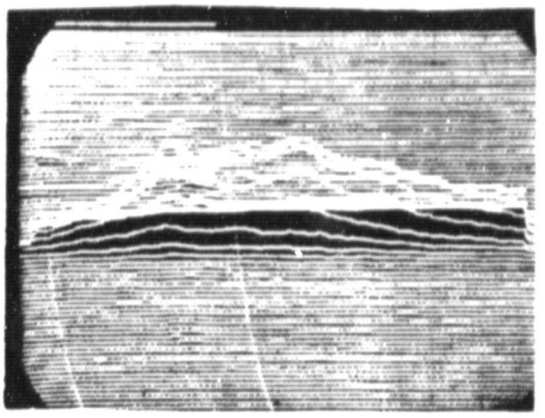

Figure 19

The spectra of 3C273. The orientation on the sky is such that the jet lies on the lower half of the picture. The exposure time is 20 minutes. The horizontal jagged lines are bad pixels with very high signal.

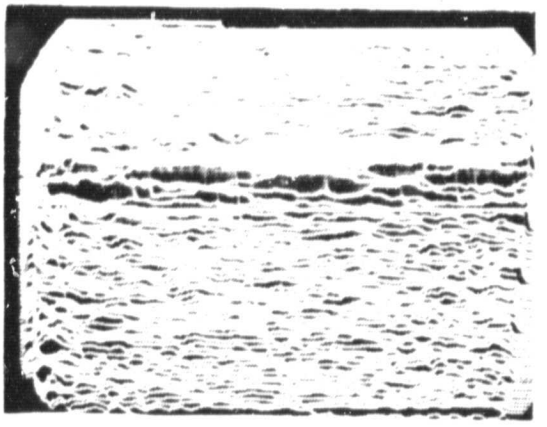

Figure 20

Rotated spectrum of 3C273, 20 minute exposure. The left side is a quantization to give full field and the right side is a linear representation of a quantization such that the gain is larger by 8. The latter shows the noise in the sky.

in Figure 21. The possible dynamic range on this exposure was 2,000 while the observed dynamic range (using the peak of the central star) was 950.

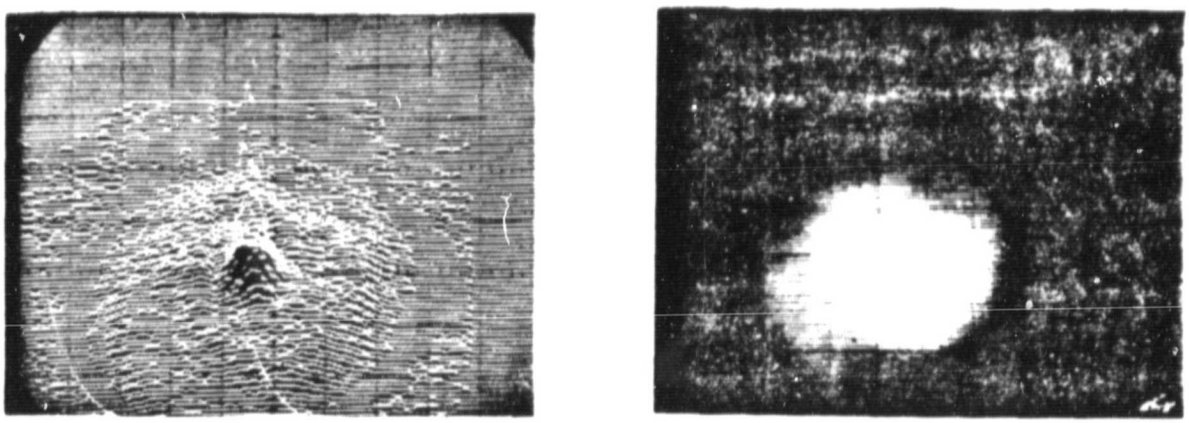

Figure 21

Planetary Nebula NGC 2343 in broadband exposure.

Certain strips through the nebula will be studied in the imaging spectrophotometric mode. This yields the intensity at a variety of different spatial points in the nebula formany different emission lines, both strng and weak. This permits the determination of electron density and the temperature of a variety of atomic species.

Finally, exposures will be obtained using the UMAP with the ICCD and a Fabrey Perot Interferometer. The latter should be

capable of distinguishing between line radiation on the distant and near sides of the nebula due to the Doppler offset. This will yield detailed information on the three dimensional structure of the nebula.

B. System Parameters - Analog Mode

In this section, we discuss the operation of the ICCD in theanalog mode. This mode was described and discussed in more detail in the main body of the proposal (p 20-22).

1. Read Noise

The random noise which occurs each time a pixel is read, or "read" noise, has been greatly reduced with the implementation of the discriminator and the 10 bit A/D converter which are mounted within the camera head. This greatly improves the shielding from external noise source. Current methods of evaluating the read noise gives numbers in the range of 35 to 50 electrons, depending upon the operating mode and the CCD. This results in analog mode performance which is better (by almost a factor of seven) than that discussed in the main proposal.

2. Maximum Value of Pixel Exposure

For most of the illustrated exposures, the brightness in the analog exposure was not at the maximum brightness level of the analog operation. However, the exposure of Figure 21 is in the analog mode and illustrates a possible dynamic range of about 2,000. Likewise, the exposure (Figure 22) of reference stars show a similar dynamic range. In these cases,the dynamic range is an "intra-scene" dynamic range, that is,the difference between the noise in the sky and the brightnessof the object.

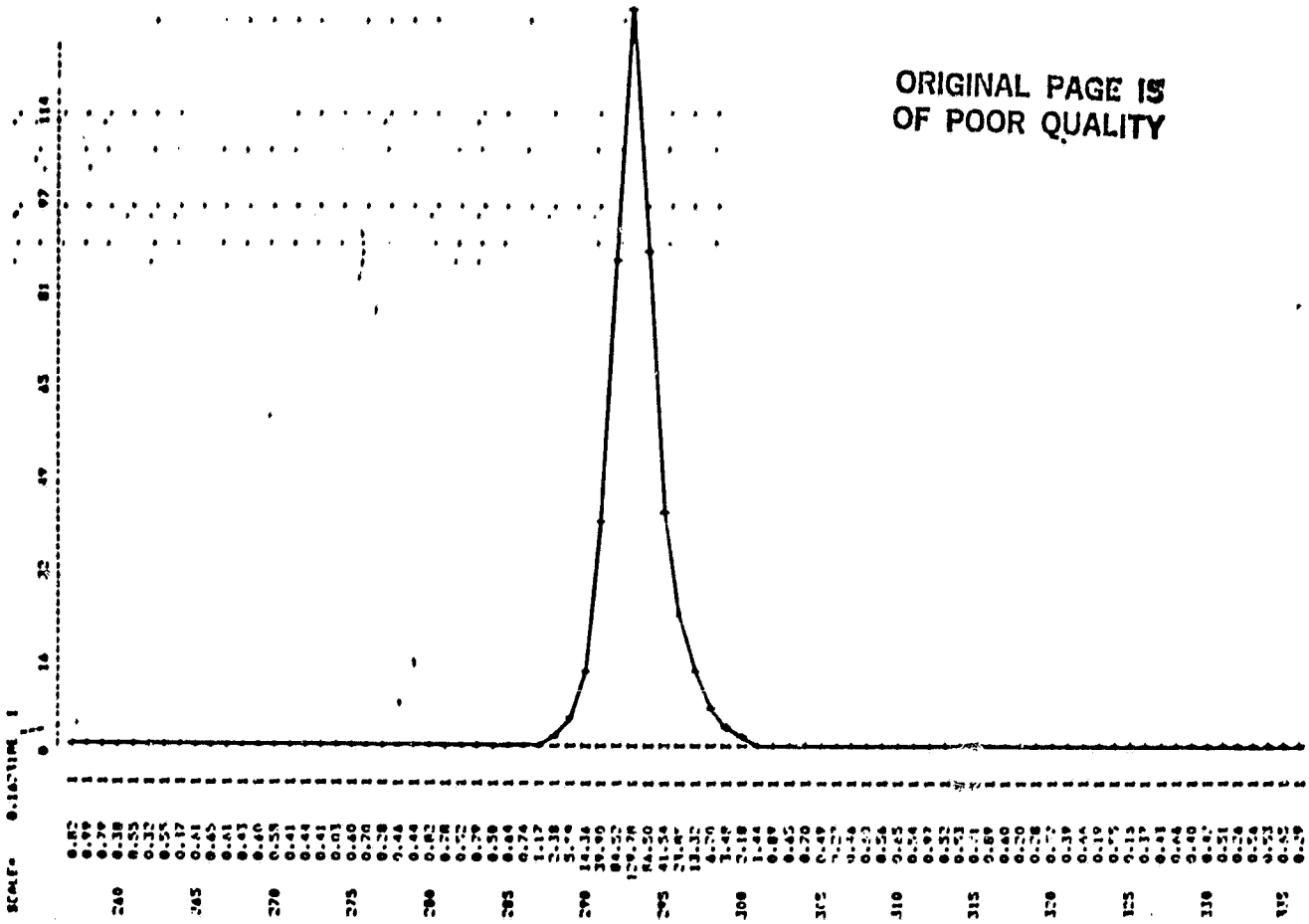

Figure 22

An exposure of a reference star, displayed in the square root display so that equal increments represent equal amounts of photon noise.

This Figure shows the uniformity of the background. It alsoillustrates the accuracy of the subtraction of leakage currentin the analog mode.

C. System Parameters - Photon Counting Mode

A general discussion of the photon counting mode may be foundin the proposal (page 7, as well as page 13, 15). We will now discuss some of the parameters of this system as measured in the January 1979 observing session. This data is still in the initial process of being reduced,

since many of the reduction programs are being developed at this time.

1. Dark Count Rate

The two primary contributions to the dark count rate arise from photons which are thermally ejected from the photocathode (and we also include in this category cosmic ray effects at the photocathode) and what shall be called "electronic dark counts" which are generated when the random noise has a large excursion and trips the discriminator. Cosmic rays which impinge on the CCD will be listed in a later category. However, for most of our discussion, we shall not distinguish between the photocathode and electronic dark counts.

As discussed above, the "read" noise is very small compared to the signal generated by a single photoelectron. This is even true given the fact that we were operating at an unusually low accelerating voltage (13.5 kv) due to the ion damage problem which is discussed in the next section. This low "read" noise results in a very low "electronic dark noise. The observations which will be used to evaluate this dark count rate are those made in conjunction with the exposure for 3C273 (Figure 20). This series, in which the shutter was controlled by the computer, consisted of a series of open and closed shutter operations. Each of these was four minutes in length, for a total of 8 exposures. One of the dark exposures is shown in Figure 23. Excluding the bad pixels and the boundary, this leaves 9,000 active pixels from the total of 10,000. In these, there were a total of 94 photoelectrons in the four minutes of exposure for a mean dark count rate per pixel of one count per 6.5 hours. This analysis includes some bad pixels which do not

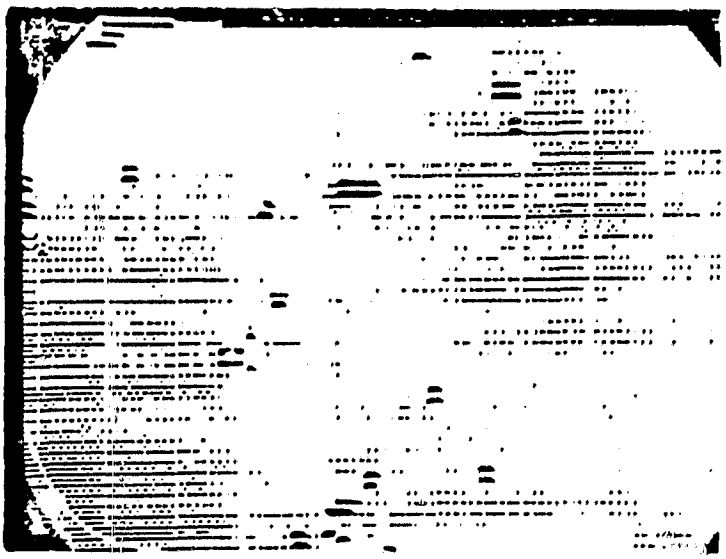

Figure 23

This is a three dimensional representation of the dark counts on a four minutes exposure with no light. Each "bump" is a single photoelectron. The doubling of these photoelectrons is not real but an artifact of our early processing programs, The "bad pixels" have been removed from this display, so the indicated counts are actual dark counts.

appear in Figure 23 and is thus a quite conservative estimate. A detailed analysis is in progress with auxiliary data to evaluate whether these were primarily thermal photoelectrons, electronic dark noise or cosmic ray events.

2. Dynamic Range

As a result of the measurements described in the above discussion, both the dynamic range and the ratio of the mean dark current and the maximum count rate, will depend on the maximum rate. Again referring to the image of 3C273, some of the bad pixels were counting at a rate near saturation. This results in a ratio between the maximum rate and the dark rate of 2.23×10^6. If

we take the dynamic range as the ratio of maximum signal to r.m.s. noise, it is 155,000. The count rate on the spectrally dispersed QSO core was significantly lower than the maximum count rate (see discussion below). Using this as the observed maximum rate, the pixels in the case of the QSO are brighter by a factor of 8100 than the observed mean dark rate.

(a) Realistic limits on dynamic range

There were other effects which limited the intra-scene dynamic range to a lower value. These consisted of the sky background for operation in the direct imaging mode and internal scattering within the spectrograph for the spectrophotometric mode. It is now believed that a large portion of the latter effect can be corrected before the next observations.

D. Current Operational Difficulties

In this section, we discuss the current difficulties as theyaffect the observational results.

1. Primary Difficulty

The primary difficulty, which will be discussed in more detail in II.A is the low quantum efficiency of the tubes. Due to gas problems, this was a fraction of one percent quantum efficiency. This means that the observation times have not resulted in as faint a limiting magnitude as expected.

2. Damage Spot

In initial testing of the ICCD tube, one region was damaged by the electrons generated by the gas ions. This may be seen in Figure 3. For some settings of the discriminator, this appears as a dark count zone.

3. Saturation of Discriminator

Improper time constants in the photon counting discriminator lead to a "horizontal bloom" for the highly saturated bad pixels. This should be able to be readjusted.

4. Clouds

The last run, for which intensive preparations were made to test the UMAP system, had severe weather problems. During a twelve day session on two telescopes less than 1.5 nights were usuable at all with serious clouds even in this interval, limiting performance and significantly brightening the night sky.

VII. CONCLUSION

In this section, we briefly review the results of this effort and qualitatively relate them to the use of this sensor for astrophysical observations.

A. Damage Measurements

The objective of the damage measurements were to quantify the damage levels produced by the photoelectrons. The importance of this damage depends upon the observing system used. There are radical difference in the requirements of a unsubtracted photon counting system, a subtracted photon-couting system, and an analog system. Thus, the purpose of these measurements was to porvide, in an astrophysical context, the expected damage levels. These are discussed in detail in the section as a function of dose and measured units and approximate discussions in terms of input photoelectrons.

As expressed in this discussion, the damage procedure is rather complex and not a simple linear phenomenon (except at low levels).

However, from the point of view of analog operations and subtracted photon-counting operations, the damage rate and resultant life-time is significantly less than channel plates operating at a photon-counting gain. As a result, it is a system which is useful for faint astrophysical objects for a large number of exposures. However, other types of applications will, or may, quickly be limited by the life-time. This life-time is expressed in number of counts or amount of light detected.

B. Annealing

Annealing is the procedure by which the increased leakage current caused by electron bombardment may be reduced. Tests were conducted on

the reduction of this leakage current by bombardment of the Charge Coupled Device with accelerated electrons in the absence of clock voltages. This procedure indeed reduced the leakage current and thus indicates a possible candidate for reducing or eliminating the detrimental effects of photoelectron damage. However, only a single cycle was tested and further work must be done in order to validate this procedure and establish optimal techniques for its use. The reproduceability, limiting values, and CCD operation after annealing were not evaluated.

C. ICCD Fabrication

Operable tubes were obtained under this contract and tested. However, the quantum efficiency has been low and the primary hope for a useful device rests in experience gained with the space telescope developments.

D. Background Subtraction

The concept of background subtraction consists of the use of an external memory to correct for the intrinsic and damage induced background leakage in order to permit a discriminator mode for photon detection. In order to evaluate this phenomenon, a computer treatment of CCD and ICCD data was performed. In addition, a prototype hardware implementation of this scheme was defined, developed and tested. This illustrated the feasibility of such subtraction.

A separate memory to store photo counts was also developed. This Circulating Semiconductor Memory (for use in a different purpose than the above) was fabricated and tested. This was developed in a manner to provide power levels that were compatible with spacecraft use. This system has worked well and has been in use at the observatory.

E. Field Use

The system has been operated in the field with a partial objective to determine any anomalous phenomena which might occur. In general, the damage appears in a similar manner and showed the kinds of difficulty which are expected. Probably the most serious difficulty is the ease of providing a relatively large dose.

F. Digital/Analog Mode

Digital/Analog mode was evaluated although this is not operating on single system. Various subaspects of this were confirmed.